A Foundation Model for Accurate Atomistic Simulations in Drug Design

Thomas Plé,[1, a)] Olivier Adjoua,[1] Anouar Benali,[2] Evgeny Posenitskiy,[3] Corentin Villot,[3] Louis Lagardère,[1,4] and Jean-Philip Piquemal[1,4, b)]

[1)] *Sorbonne Université, LCT, UMR 7616 CNRS, 75005 Paris, France.*

[2)] *Qubit Pharmaceuticals, Advanced Research Department, Boston, MA 02116, USA*

[3)] *Qubit Pharmaceuticals, High Performance Computing Unit, 75014 Paris, France.*

[4)] *Qubit Pharmaceuticals, Advanced Research Department, 75014 Paris, France.*

(Dated: 9 April 2025)

Neural network potentials now offer robust alternatives to electronic structure and empirical force fields computations for the on-the-fly production of the potential energy surfaces required in atomistic Molecular Dynamics (MD) simulations. However, widespread application in Chemistry and Biology faces several challenges: the need for fast inference and economical training; stringent model transferability requirements, particularly including charged-species interactions. Trained exclusively on synthetic quantum chemistry data, FeNNix-Bio1 sets a new standard for Foundation Machine Learning Models to provide predictive condensed-phase MD simulations including quantum nuclear effects. Its full-range of capabilities is demonstrated by modelling diverse biochemical problems including water properties, ions in solution, large-scale protein dynamics, complex folding free-energy landscapes, protein-ligand binding free energies and chemical reactions. FeNNix-Bio1 is accurate and systematically improvable while limiting human parametrization efforts: it is likely to have a strong impact in Drug Design.

I. INTRODUCTION

With the recent releases of the AlphaFold[70] and RoseTTAFold[8] protein structure foundation models, artificial intelligence (AI) has revolutionized protein science enabling *in silico* prediction of crystal structures. However, protein folding is only one of the many aspects of the physical processes required to be modeled if one wants to deal with the complex problem of drug design. Indeed, proteins' structures are not static and dynamically change over time while interacting with drugs, ions, water solvent, and other biomolecules of the chemically reactive cellular environment. Therefore characterizing the structural dynamics of complex biological systems remains a major challenge that has yet to be fully addressed by AI through the introduction of a foundation model dedicated to atomistic Molecular Simulation. Indeed, up to now, the Molecular Dynamics (MD) approach[3,100] remains the method of choice to unravel the biomolecular dynamics. The application of atomistic MD to drug design requires to solve Newton's equations of motion to predict the atomic movements over time. Such a resolution being grounded on physics, it requires the use of a numerical model describing the interatomic interactions associated to the system quantum potential energy surface. Ideally, MD simulations should therefore be grounded on quantum mechanics and allow for chemical reactivity. However, despite the rise of Density Functional Theory (DFT)[77] and the availability of highly scalable simulation methods and codes[26,63,80,95], ab initio MD (AIMD) simulations' computational cost remains prohibitive for biophysical and drug design applications due to the size of the systems at stake and the associated long biological timescales. Thus, in practice, interatomic potentials rely on more computationally tractable parametric equations known as empirical force fields (FFs)[91]. Biosimulation force fields' parametrization has been continuously refined and evolved over the years starting from the popular "fixed charge" non-polarizable FFs (NPFFs) models [69,149,155], reactive non-polarizable FFs (RNPFFs)[84,134], up to polarizable FFs (PFFs) ones[67,101,136]. Among these latter, quantum-inspired polarizable potentials[39,53,107,122,168] can approach ab initio quality but their applicability strongly depends on the complexity of the system under study as the increased functional form sophistication de facto limits their speed and scalability. In that context, faster intermediate polarizable approaches became popular, presenting a more favourable balance between accuracy and computational cost, while being suitable for large-scale and free energy simulations [86,89,99,106,109,118,124] thanks to the availability of massively parallel GPU-accelerated implementations [2,27,81,113,144,148]. In practice, PFFs do provide a viable solution to accurate molecular dynamics simulations but, compared to AIMD, they remain limited by their absence of modeling of chemical reactivity and, despite the existence of semiautomated strategies[36,154,158], they inherited the tedious FFs parameterization process that still requires significant human efforts. If Machine Learning (ML) is a promising route to fully automate the PFFs parametrization process (see for example reference[28]), neural networks have emerged as a complete new – AI-based – independent strategy capable of powering molecular simulations.

Indeed, neural network potentials (NNPs) have been shown to embody many advantages compared to traditional approaches as they are highly flexible and do not

[a)] Contact author: thomas.ple@sorbonne-universite.fr

[b)] Contact author: jean-philip.piquemal@sorbonne-universite.fr

require to derive a complex physically-inspired functional form. By design, their parametrization is automated and only requires the availability of large *ab initio* computations databases. With the right amount of data, they can be extremely accurate, do not suffer from limitations in terms of target systems and can handle chemical reactivity. Overall, such approaches could offer a viable route for molecular simulation going beyond FFs and AIMD. Of course, many parameters govern the applicability of NNPs such as their intrinsic neural architectures designed to map quantum data. In practice, compared to AlphaFold/Rosettafold approaches, other choices of deep learning techniques are possible that go beyond the use of the popular but computationally challenging large language (LLMs)[21,65] and diffusion models[127,160].

Indeed, the discussion of the application of Neural Networks to molecular dynamics started with the introduction of approaches including the Behler-Parinello [12] (BPNN) and the Gaussian Approximation Potential[9] (GAP) architectures. Since then, numerous computational strategies have been proposed[9,11,12,18,31,49,52,56,57,90,104,119,131,132,135,138,146,163,171]. Overall, NNPs and their associated quantum chemistry datasets such as ANI-2X[35] or AIMNet[172] are becoming popular in chemistry as they provide quantum chemistry -accurate results for gas phase small molecule simulations at a largely reduced cost compared to standard ab initio computations.
Nevertheless, such approaches struggle when going beyond gas phase towards condensed phase simulations[121]. More specifically, if progresses were made in condensed phase reactivity[166], neural networks still don't reach the accuracy of the best empirical force fields for modelling the structural dynamics and properties of biological systems. Aside from the amount and the quality of the quantum data, this can be attributed to the generalization of intrinsic NNPs cutoffs that are usually chosen to be in the 4-6 Å range and which despite capturing mostly all physical effects including many-body ones (polarization and charge delocalization) fail to correctly model long-range effects such as electrostatics, dispersion etc... Various strategies of hybridization between force fields and neural networks have been proposed, mixing ML approaches with more traditional physically-motivated, i.e. FF-like, functional forms[6,22,30,61,66,75,116,120,146,147,157,161,165,168]. Among these, hybrid approaches coupling NNPs and PFFs such as the ANI2X/AMOEBA approach introduced within the Deep-HP framework[66] allow for fast and accurate ligand binding studies where the solvent-solvent and solvent-solute interactions are computed via a PFF while the solute-solute interactions are evaluated using a DNN. Such a strategy explicitly includes physical PFF's long-range interactions as well as critical biosimulation features such as polarizable solvent and ions while providing the DNN solute quantum mechanical accuracy with an overall force field cost. An essentially similar theoretical framework has been later used within the AI2BMD (AI-based ab initio biomolecular dynamics system) approach[156] for biomolecular simulations. However, because of their hybrid nature, these approaches remain non reactive despite their speed.They also strongly rely on the PFFs themselves, benefitting from the years spent in their careful development, but also require additional parametrization to be further extended.

On the software side, several libraries now facilitate NNPs implementations including SchnetPack[133], MLAtom[38], DeepMD-kit[164] or our own FeNNol[115]. FeNNol is a flexible and modular Python library with just-in-time compilation capabilities which, within the Jax framework[23,33], is able to build, train, and run atomistic ML models, with a particular focus on physics-enhanced neural network potentials. The interested reader can refer to dedicated review papers for further details about the existing architectures and models[76,114,162].

In that context, and towards extending further the applicability of pure NNPs, an international team of researchers recently pioneered the idea of a foundation model for molecular simulation with MACE-MP-0, a single general-purpose ML potential, able to tackle diverse applications in material science[10]. The MACE foundation model is at the origin of a complete family of methods capable of performing a variety of simulations of multiple atomistic systems ranging from molecules to materials and that can extend up to small proteins. If MACE-MP-0 is able to run stable molecular dynamics on molecules and materials and to predict various chemical reactions and properties, its applicability to condensed phase biosystems simulations remain limited both in term of accuracy and computational performances. A first step towards improved organic molecules modelling has been performed via the MACEOFF-23[78] potential but it is still not suitable for drug design applications. In practice, the ability of the present ML approaches to perform atomistic condensed phase molecular dynamics simulations of biological systems remain hindered by several key constraints. First, as for any method, a foundation model is required to be computationally efficient in order to access the mandatory biological timescales, making the existence of a massively parallel, GPU-accelerated, implementation of the neural network architecture key. The second architecture-related constraint concerns the need to ensure a full transferability of all type of interactions in the condensed phase including the one involving the charged-species in order to obtain faithful molecular dynamics simulations of the main building blocks of biological systems, i.e. water solvent, ions including metals, proteins, nucleic acids, sugars, membranes etc... Finally, as they are trained on large quantum chemistry database, neural networks can only reproduce the electronic Born-Oppenheimer surface and won't access meaningful condensed-phase dynamics and properties without a form of inclusion of nuclear quantum effects (NQES)[96,97,112,117]. In this paper, we introduce FeNNix-Bio1, a scalable Foundation Machine-Learning Model capable of reactive MD simulations including NQEs that intends to solve these issues. The manuscript is structured as follows: in section II, we first describe a series of application of FeNNix-Bio1 including: a study of the liquid water properties, a study of the behaviour of ions in solution, complex free-energy landscapes, accelerated reversible protein-folding, protein-ligand absolute binding free energies, various chemical reactions and several benchmarks to illustrate the performance and scalability of the approach including a simulation of the full SARS-Cov2 Spike protein with corresponding glycans and membrane. We then introduce the foundation model architecture, the dataset used for training, the training methodology itself and various key methodological aspects such as intrinsic uncertainty quantification and the application of alchemical free energy simulations in that context.

II. DISCUSSION

A. Liquid water properties

Accurate modeling of biosystems requires an excellent description of the water solvent which is known for its very complex behavior. To date, first principle simulations still attempt to recover experimental data when modelling water across its diverse phases[123]. Furthermore, accurate results require the explicit inclusion of NQEs within the dynamics coupled to the choice of an accurate DFT functional[110,126]. Alternatively, for larger scale simulations, numerous force field have been developed over the years ranging from point charges water models[1,14,15,60,62,68,72,94,150], to more advanced polarizable FFs able to capture the subtle many-body induction and charge delocalization effects present in water[24,32,43,87,88,108,120,122,125,157]. The present foundation model builds on this combined knowledge since it is grounded on a Density Functional Theory (DFT) dataset and is powered by non-classical molecular dynamics that include explicitly NQEs as initially tested on the QAMOEBA polarizable potential. We compute various water properties with FeNNix-Bio1, across a range of temperatures such as radial distribution functions, density and enthalpy of vaporization. Excellent results are obtained (see Figure 1) as the foundation model appears extremely accurate, reaching the quality of the community's most accurate polarizable models while outperforming the popular MACE-OFF neural network potentials for a fraction of the computational cost (see section III). Particularly, FeNNix-Bio1 outperforms the most accurate models on the enthalpy of vaporization, a key property describing the accuracy of a given model accross phases.

Additionally, we computed the hydration free energy of water and found a value of -6.49 kcal/mol, close to the experimental value of -6.32 kcal/mol.

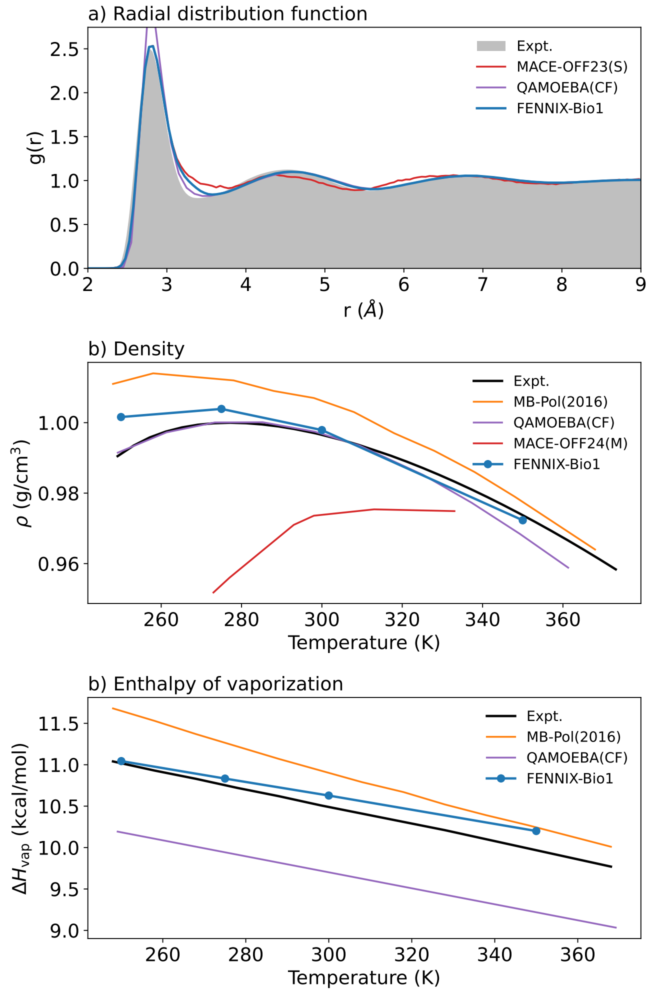

FIG. 1. Properties of liquid water; a) Oxygen-Oxygen radial distribution function at 300K. Experimental results from ref.[139]. All simulations include nuclear quantum effects via the adQTB method[92]; b) Density as a function of temperature. Experimental results from refs.[140,151]; c) Enthalpy of vaporization as a function of temperature. Experimental results from ref.[151]. Results for MB-Pol, QAMOEBA and MACE-OFF for the density and enthalpy are extracted respectively from refs.[122], [98], [78].

B. Ions in solution

Ions are ubiquitous in biochemical systems and their inclusion in molecular simulations is essential. For example, including a physiological concentration of Na+ and Cl- ions has been shown to have a significant influence on solvation and binding free energies[37]. Furthermore, some ions are key elements of specific motifs as in the case of Zinc fingers[42].

Simulating ions using NNPs historically posed severe challenges, mainly due to the non-locality of the definition of charge states[75] that conflicts with the local nature of most ML models. Consequently, the authors of MACE-OFF23 chose to exclude ions from the training set in order to maintain locality of the model[78]. On the other hand, AIMNET2[5] uses iterative non-local refinement of charges and explicit long-range interactions to accurately model charged systems, at the cost of higher model complexity and more cumbersome parallelization. As a middle-ground solution, we chose to model charge states using system composition and total charge only, as described in section V A. Geometry-dependent interactions are thus still purely local but are affected by a geometry-independent non-local charge embedding, allowing to describe different charge states of the whole system. To assess the capability of FeNNix-Bio1 to reproduce the subtle behavior of Na+ and Cl- ions in solution, we solvate separately a chloride ion and a potassium ion in a water box and compute the associated radial distribution functions between these ions and the oxygen atoms of the water molecules. We compare these with the same properties obtained with the AMOEBA-03[58] force field and the Amber99[153] force field (combined with TIP3P water for the latter) and find a good agreement between these situations, with a clear shell structure around the monovalent ions as shown in Figure 2. We observe a slight (0.15Å) systematic shortening of the caracteristic distances of the first shell in the FeNNix-Bio1 simulations. Interestingly, such shorter distances were also observed for the chloride anion in ab initio simulations[51]. Additionally, we compute the hydration free energies (by leveraging the Lambda-ABF alchemical method[4,82]) of the same ions (presented in Table I) and obtain results with AMOEBA and Amber, showing that the structure and the thermodynamics of these solvated systems is well reproduced by our ML model.

	FeNNix-Bio1	AMOEBA-03	expt.
Na	-90.5	-89.9	-88.7
Cl	-83.4	-84.6	-89.1

TABLE I. Hydration free energies of Na and Cl ions, in kcal/mol. AMOEBA-03 results from ref.[58]. Experimental values from ref.[130]. 1.9 kcal/mol was added to calculated results to match experimental conditions[58].

C. Torsional free energy landscape of alanine dipeptide

Over the years, the two dimensional free energy landscape associated with the (ϕ,ψ) Ramachandran angles of the alanine dipeptide has become an elementary benchmark of the capability of an atomistic model to reproduce basic amino-acid interactions and structure. As such, it is a mandatory intermediate step towards a complete protein force field[116]. Here, we compute the free energy surface of interest by running two dimensional Adaptive Biasing Force (ABF) simulations both in gas phase and in condensed phase with explicit solvent. Interestingly, FeNNix-Bio1 is in agreement with AMOEBA[137] in the condensed phase and closer to Amber99 in the gas phase. This change of the torsional free energy surface is consis-

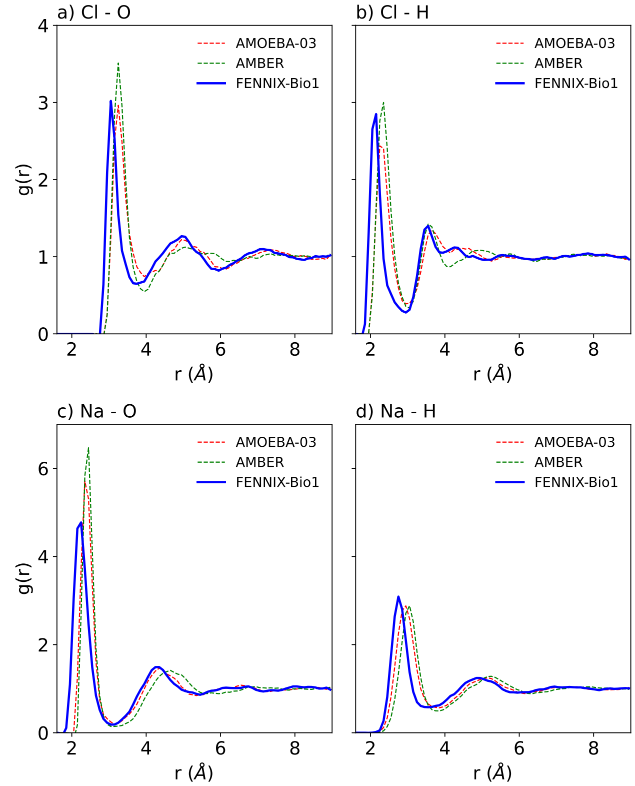

FIG. 2. Radial distribution functions of Na and Cl ions in water at 300K.

tent with MP2/implicit solvent results[159] and illustrates the good transferability of FeNNix-Bio1 from gas to condensed phase (see Figure 3)

D. Accelerated reversible folding of the Chignolin protein

To further validate our model in a realistic biochemical framework, we study the reversible folding of the chignolin CLN025 (PDB ID:1UAO). Even if it is known in the literature as a fast folding process into a β-hairpin, the associated time is in the microsecond range[85]. Furthermore, a complex free energy landscape is known to be associated to this process with three well separated metastable states: a folded, a misfolded and an unfolded one[48]. Leveraging the coupling between DeepHP and the Colvars library[45,46], we recover it by running enhanced sampling multiple-walker well-tempered meta-abf[47] simulations of the system with two distance-based collective variables: the hydrogen bond distance between Asp3O and Tyr7O and the hydrogen bond distance between Asp3N and Tyr8O. Such simulations used 4 walkers for 100ns each for a total of 400ns. FeNNix-Bio1 is able to recover the 3 aforementioned states with free energy minima at the expected pair distance values. The AMBER99 force field also recovers them but with a steeper free energy surface surrounding them. Interest-

why?

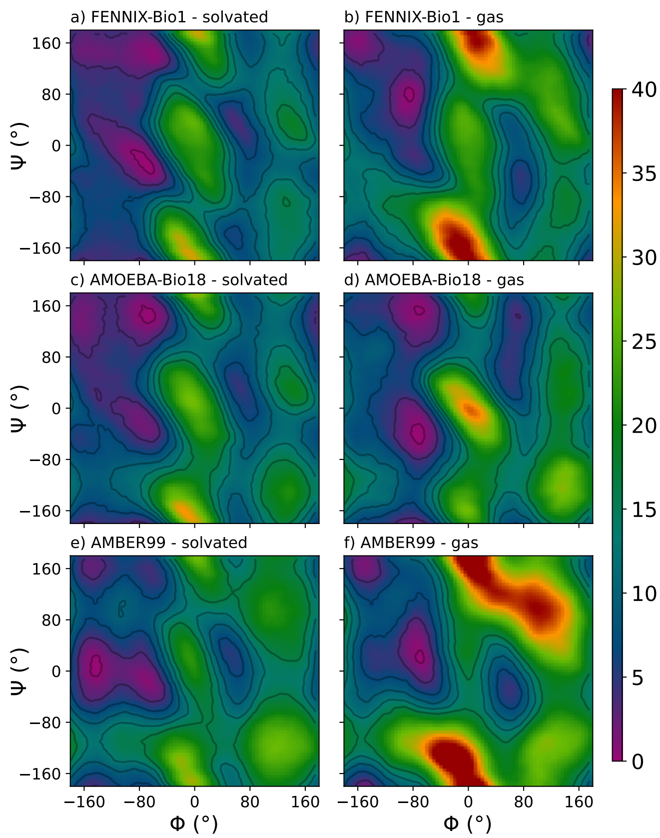

FIG. 3. Torsional free energy profile of solvated and gas-phase alanine dipeptide at 300K computed with a-b) FeNNix-Bio1(S), c-d) AMOEBA-Bio18 and e-f) AMBER99. Energy units in kcal/mol. Contour levels are linearly spaced from 0.5 to 16 kcal/mol.

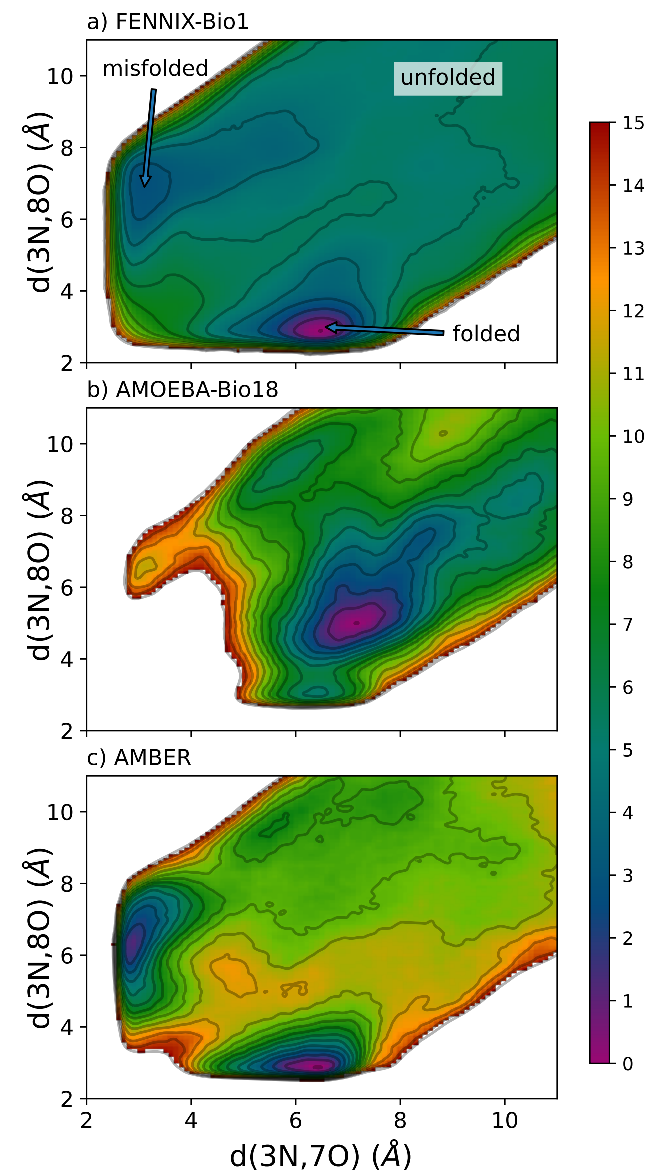

FIG. 4. d(3N,7O),d(3N,8O) free energy profile of the Chignolin protein (PDB 1UAO) with explicit solvent at 300K computed with a) FeNNix-Bio1(S), b) AMOEBA-Bio18 and c) AMBER. Energy units in kcal/mol. Contour levels are linearly spaced from 0 to 15 kcal/mol. Energies above 15 kcal/mol are clipped.

ingly, AMOEBA only finds one global minimum corresponding to neither of the expected ones. Previous studies tackling this system with a ML model were limited to non-transferable protein models with solvation effect taken into account via an embedding with a traditional force-field[156]. To the best of our knowledge, this is the first time that the reversible folding of a protein is computed with a universal machine learning model.

E. Phenol-lysozyme complex, absolute free energy of binding

Modelling the binding between small molecules and a macromolecular target has become a fundamental tool for computational drug design. Here, we focus on the complex formed by the polar phenol ligand bound to a Lysozyme mutant (L99A/M102H) which has been extensively studied with traditional approaches before[34,129]. In a first step, after standard equilibration, we monitor the evolution of the RMSD of the protein and observe stable evolution of its backbone as can be seen in Fig 5. Following the protocol described in ref[82] we define a DBC (Distance-to-Bound-Configuration) collective variable[128] associated to the binding mode of phenol, showing a unimodal distribution as seen in Fig 5 . To compute the absolute binding free energy of the complex, we leverage alchemical methods that rely on the sampling of an unphysical path where the interactions between the ligand and its surroundings are progressively turned off, first in its bound state and also in the bulk. The free energy of interest is recovered through a thermodynamic cycle. To the best of our knowledge, this is the first time that such a quantity is obtained with a Machine Learning Potential. Using Lambda-ABF in combination with DBC restraints[82], we obtain a value for the standard absolute binding free energy of -5.5 kcal/mol, within 1 kcal/mol of the experimental value of -5.44 kcal/mol[102].

Note that during this process, we compute the hydration free energy of phenol and find a value of -6.8 kcal/-mol, in good agreement with the experimental result of -6.62 kcal/mol[29].

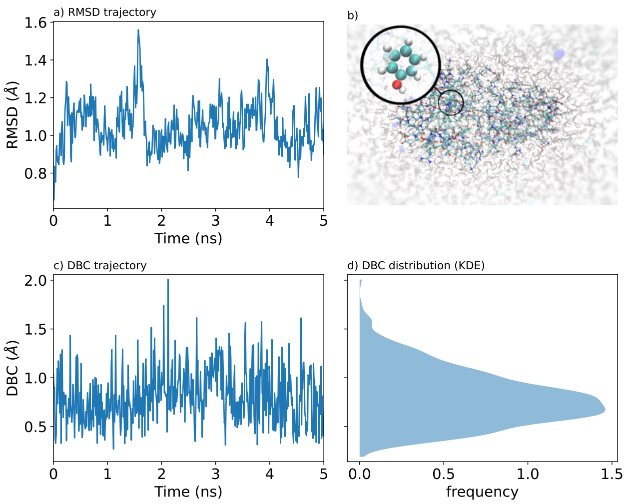

FIG. 5. a) Trajectory of the Lysozyme protein's backbone RMSD. b) Ball and stick representation of the phenol-Lysozyme complex in solution. c) Trajectory of the ligand's DBC. c) Kernel Density Estimation of the DBC distribution during the trajectory.

Complexation	Solvent	Restraint	Total	Expt.
-17.6	6.8	5.3	-5.5 ± 0.5	-5.44

TABLE II. Standard absolute binding free energy of phenol to Lysozyme and free energy components of the thermodynamic cycle. "Complexation" corresponds to the free energy difference between the fully interacting complex and the non-interacting complex with DBC restraint. "Solvent" corresponds to the negative hydration free energy of phenol. "Restraint" is the free energy associated to the release of the DBC restraint. All free energies in kcal/mol.

F. Chemical reactivity: Butadiene to cyclobutene gas-phase reaction

One of the most paradigm-shifting features of MLPs is their ability to systematically model chemical reactivity[162], which was traditionally reserved to ab-initio, semi-empirical or very specialized force fields[134]. In this section, we explore the free energy landscape for the conversion of butadiene to cyclobutene in the gas-phase, a well-studied chemical reaction[7,59,64]. we show that FeNNix-Bio1 is able to semi-quantitatively model the reaction out-of-the box, efficiently sampling physically relevant reactive pathways. We also show that fine-tuning allows a systematic convergence of the free-energy barrier of reaction to with very small amounts of data.

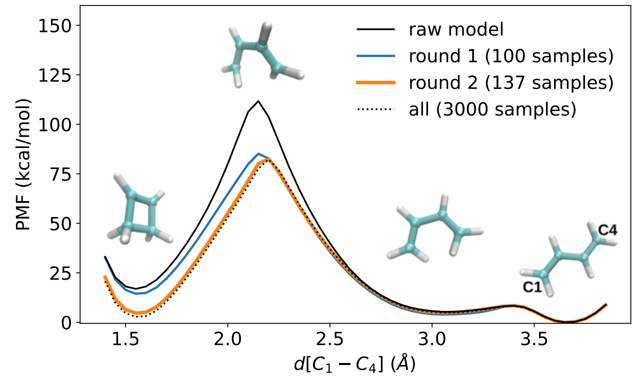

FIG. 6. Potential of mean force of the cyclobutene ↔ butadiene reaction as a function of the C1-C4 distance for different rounds of finetuning. The "raw model" (black curve) corresponds to out-of-the box FENNIX-Bio1, "round 1" (blue curve) corresponds to the PMF estimation after a first round of finetuning using 100 samples, "round 2" (orange curve) corresponds to the second round of finetuning with 137 samples, "all" (dashed curve) corresponds to a model finetuned on all the 3000 gathered samples.

To study the reaction from butadiene (on the right of figure 6 to cyclobutene (on the left of figure 6) in the gas phase, we perform an accelerated MD simulation via metadynamics, starting from butadiene (*trans*) using the $C_1 - C_4$ distance as collective variable. We use an aggressive setup for the metadynamics to quickly cross reaction barriers and reconstruct the potential of mean force (PMF) from the generalized force stored on a unidimensional grid using the Colvars[45,46] program coupled with Tinker-HP[2,81]. Within a few tens of picoseconds of simulation, we obtain a first reaction path to cyclobutene. We reconstruct the full PMF shown in figure 6 (solid black curve) from 1 ns of simulation.

We then assess the confidence of the model by evaluating its ensemble variance (see section V for implementation details) on 3000 points sampled from a secondary Umbrella sampling simulation (in order to obtain an even distribution of points along the collective variable). From this simulation, we can first validate that FENNIX-Bio1 really models a reorganization of the bond orders in the carbon chain when crossing the barrier. Indeed, as shown in Figure 7,a), the difference of distances $\Delta d = d(C_1 - C_2) - d(C_2 - C_3)$ between the first two carbon bonds is negative to the right of the barrier and positive to the left, indicating an inversion of bond orders when going from the linear butadiene to the cyclic cyclobutene. This behaviour is expected from basic chemical intuition and was confirmed numerically, for example in ref.[7].

Figure 7,b) shows the predicted uncertainty as a function of the collective variable. As expected, the model displays much higher uncertainty in the region of the reaction barrier. In order to refine our estimate of the free-energy barrier, we subsample configurations for which we compute the ab-initio energy and forces and that we use to fine-tune the model. We thus start by selecting 50 points uniformly in our sample and 50 other points with uncertainty greater than 1.2 kcal/mol. Among these 100 points, we keep 10 as a validation set. We finetune the model for 5000 epochs using the AdaBelief optimizer with a constant learning rate of 1e-5. We freeze all paramters except weights and biases in multi-layer perceptrons associated to C and H species. The loss function for finetuning is composed of a MSE term for forces with a weight of 1000 and a CRPS term for relative energies (with respect to the lowest energy point sampled in the steered MD run) with a weight of 10.

After finetuning, we simulate again the system with the same metadynamics setup and obtain the blue curve of figure 6. We see that the main effect of the finetuning was to reduce the free-energy barrier from 110 kcal/mol to 84 kcal/mol. The free energy difference between butadiene and cyclobutene is also slightly shifted down, from 16.5 kcal/mol to 14 kcal/mol.

We then evaluate the uncertainty of the finetuned model on the previously gathered conformations and selected the 37 points with an uncertainty higher than 0.5 kcal/mol. These points are mainly located on the butadiene side of the barrier. We then finetune again the original model using the 137 configurations. After this second round of finetuning, the free energy barrier barely changes but the free energy difference between the end states shifts down again to 4.5 kcal/mol. As a verification of convergence, we finetuned the model on all the 3000 conformations gathered in the first run and see no significant further modification of the free energy landscape (dashed curve of Figure 6).

This experiment on a simple reaction clearly shows the relevance and data-efficiency of the finetuning strategy starting from our foundational FeNNix-Bio1 model, illustrating its capacity to be systematically improved.

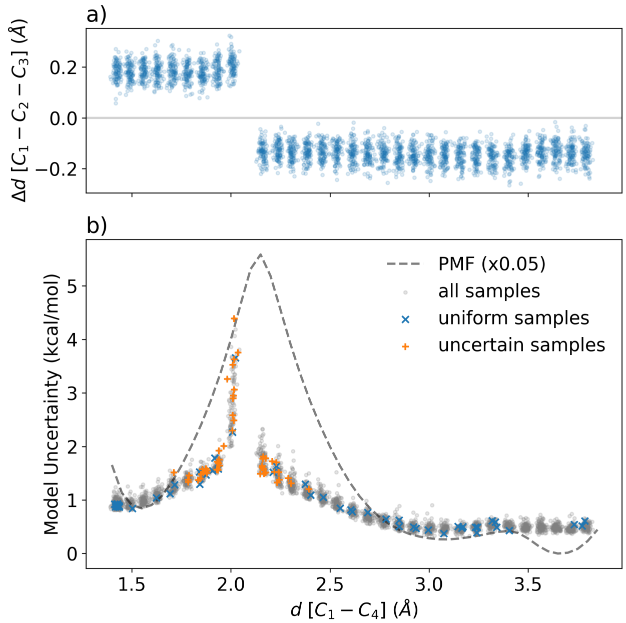

FIG. 7. a) Difference of distances $\Delta d = d(C_1 - C_2) - d(C_2 - C_3)$ as a function of the $C_1 - C_4$ distance for points sampled during an Umbrella sampling of the butadiene to cyclobutene conversion. b) Model uncertainty for points sampled along the Umbrella sampling run. The samples selected for finetuning the model are highlighted in blue (uniformly sampled) and orange (uncertain samples). The PMF computed with the raw FENNIX-Bio1 model (scaled by a factor 0.05) is superimposed (dashed line) for reference.

System	# atoms	peak perf.	# GPU
watersmall	648	91	1
waterbox	1500	70	1
waterhuge	12000	38	1
DHFR	23558	18	1
puddle	96000	2.2	1
lake	288000	1.4	16
Spike	1658576	1.3	64
bay	2592000	1.2	64
sea	7776000	1.2	128

TABLE III. Peak performance (in million steps/day) for different system sizes simulated with the FeNNix-Bio1 model. The number of GPUs used to obtain the peak performance is indicated in the last column.

III. COMPUTATIONAL PERFORMANCE

We evaluated the performance of FeNNix-Bio1 on the HXM5 H100 Nvidia GPUs of the Jean-Zay supercomputer center of IDRIS, each of them embodying 80G of memory. The nodes of Jean-Zay are made of 4 of these GPUs, communicating through a 100 GB/s Intel Omni-Path interconnect. The systems used and the number of atoms they are made of are listed in Table III, they range from a small water box of 216 molecules (648 atoms) up to a more than 7 millions atoms water box. We also ran simulations with the closed structure of the Spike glycoprotein of Sars-Cov2 in combination with the corresponding membrane (PDB: 6VXX), showcasing real-life biomolecular complexes of such sizes[20].

The smaller systems (from "watersmall" to DHFR) were run through the molecular dynamics engine of the FeNNoL library[115], while the largest ones (starting from "puddle") leveraged the interface of FeNNol and Tinker-HP through Deep-HP[66]. This interface enables efficient computation of neighbour lists and parallel multi-GPU simulations through the native 3D domain decomposition included in Tinker-HP. Note that the multi-GPU capabilities of Deep-HP for message-passing models is still experimental and thus not fully optimized. In particular, messages between atoms in neighbouring domains are re-computed on each GPU, rather than communicated which imposes overlapping computations for all atoms within the receptive field of the model (11Å). Future work will focus on further integration of FeNNix-Bio1 within Tinker-HP to improve scalability. Details of the setup used to produce these numbers are given in Supplementary Informations.

Notably, we observe more than one order of magnitude better performance for FENNIX-Bio1 compared to the smallest of the MACE-OFF models and two orders of magnitude better performance for the largest of the MACE-OFF models. Note that all simulations were performed using a common JAX implementation of the models and MD engine, enabling a fair comparison. The optimized CUDA implementation of MACE proposed in ref.[78] suggests a speedup by a factor of two compared to our JAX implementation, still far from bridging the gap compared to FENNIX-Bio1.

The fast inference speed of FENNIX-Bio1 – which is in the range of optimized polarizable force fields – enables its use for real-life production simulations of bio-physical systems.

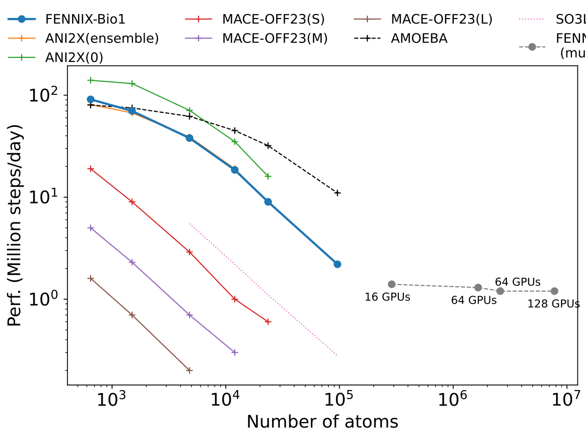

FIG. 8. Performance (in million simulation steps per day) for various system sizes on NVIDIA H100 80GB GPU(s). FENNIX, MACE and ANI2x calculations performed with FeNNol's JAX implementation of the models. Systems above 10^5 atoms simulated using deep-HP[66]. When not explicitely indicated, single-GPU performance is reported. SO3LR performance extrapolated on the basis of 3.25×10^6 s/atom/step as reported in ref.[71].

IV. CONCLUSION AND PERSPECTIVES

We presented the FeNNix-Bio1 machine learning foundation model for biosimulations. The approach is able to tackle diverse applications in drug design ranging from biology to chemistry and providing an accurate and computationally tractable alternative to modern force fields. Its applicability to a diversity of complex systems bypasses the parametrization process of traditional approaches, plaguing drug discovery in term of human efforts. FeNNix-Bio1 is solely grounded on synthetic quantum data (energies and forces) thanks to its associated quantum chemistry database. FeNNix-Bio1 is shown to be systematically improvable as the dataset enlarge and finetuning strategies will allow to orient the dataset growth towards maximizing the model accuracy in relevant area of chemical space. If the present dataset was grounded on DFT, we are currently working on a post Hartree-Fock version to push further the model towards the absolute 1 kcal/mol chemical accuracy limit. In that regard, our developed Ocean dataset that uses pseudopotentials, will be an asset to capture the key valence correlation effects using advanced quantum chemistry methods capable of approaching Full-CI (CI=Configuration Interaction) in the complete basis set limit (CBS). This will also include quantum computing ansätze for chemistry[145] and our global strategy will be able leverage Fault Tolerant Quantum Computing (FTQC) algorithms once hardware is available[73,167]. Moreover, current scalability and computational resources of this first model are already in the range of production polarizable force fields. Further high performance computing optimizations enabling to reduce the overhead of automatic differentiation and MD acceleration techniques will essentially nullify this gap, especially for large systems since NN offer diminished communications on large exascale computing systems compared to standard FFs. Presently, the approach can already be used in synergy with the various enhanced sampling techniques present in Tinker-HP. FeNNix-Bio1 is likely to have a strong impact on drug design as it can be directly used with the outputs of both AlphaFold/RosettaFold-like protein prediction frameworks and small molecules (and beyond) generative modelling[19] models.

V. METHODS

A. Model Architecture

In FeNNix-Bio1, the total energy is decomposed into atomic contributions and expressed as the average over a shallow ensemble[74]:

$$E_{\text{tot}} = \sum_{i,j} E_{\text{ZBL}}(r_{ij}) + \frac{1}{N_{\text{ens}}} \sum_{j=1}^{N_{\text{ens}}} \sum_{i=1}^{N_{\text{at}}} \left[MLP_E^{G(Z_i)}(x_i) \right]_j \tag{1}$$

where E_{rep} is the Ziegler-Biersack-Littmark (ZBL) screened nuclear repulsion[170]:

$$E_{\text{ZBL}}(r_{ij}) = \frac{Z_i Z_j}{4\pi\epsilon_0 r_{ij}} \sum_{n=1}^{4} c_n e^{-\alpha_n \frac{r_{ij}}{d}(Z_i^p + Z_j^p)} \tag{2}$$

with Z_i the atomic number of atom i, r_{ij} the distance between atoms i and j and c_n,α_n, d and p trainable parameters that are initialized to the values provided in ref.[170].

$MLP_E^{G(Z_i)}$ is a multilayer perceptron outputting N_{ens} scalars that are interpreted as an energy distribution.

More precisely, MLP_E is a mixture-of-experts model[25] where the routing is performed based on the chemical group of each atom $G(Z_i)$. The chemical groups that we define split the periodic table into families of similarly-behaved elements (see details in Supplementary Information). This grouping is more parameter-efficient than fully element-specific networks, and is more flexible than purely universal networks while still allowing to share information between chemical species.

The atomic embedding x_i which is fed into MLP_E is a vector of size N_f describing atom i in its environment and is obtained via a two-layer message-passing graph neural network. In a first step, the chemical species of atom i is encoded into a vector e_{Z_i} using its neutral isolated atom electronic structure as described in ref. 146. The total charge Q_{tot} of the system is then encoded using a procedure similar to the neural charge equilibration proposed in ref. 173:

$$q_i, \tilde{f}_i = MLP_Q(e_{Z_i}) \tag{3}$$

$$f_i = \log\left(1 + e^{\tilde{f}_i}\right) \tag{4}$$

$$e_{Q_i} = q_i + \frac{f_i}{\sum_{j=1}^{N_{\text{at}}} f_j}\left(Q_{\text{tot}} - \sum_{j=1}^{N_{\text{at}}} q_j\right) \tag{5}$$

In eq. (3), q_i and s_i are both N_Q dimensional vectors and we perform the neural charge equilibration independently over the N_Q channels. The vector e_{Q_i} then contains N_Q "distributed charge hypotheses" that encode how the electrons in the system distribute between the chemical species that are present. Note that while this encoding is completely non-local, it does not involve atomic coordinates which is key to the numerical efficiency and parallelizability of the model. This charge encoding strategy is similar to the one proposed in ref.[146] that has been used in the recent SO3LR model[71].

The initial embedding $x_i^{(0)}$ is then obtained by combining the information from e_{Z_i} and e_{Q_i} as:

$$x_i^{(0)} = LN(MLP_0(e_{Z_i} \mid\mid e_{Q_i})) \tag{6}$$

where $||$ represents vector concatenation and LN is the layer normalization operation defined as:

$$\forall y \in \mathbb{R}^d, [LN(y)]_k = \frac{[y]_k - \bar{y}}{\sqrt{\sum_{k'=1}^{d}([y]_{k'} - \bar{x})^2/d}} \tag{7}$$

with $\bar{y} = \sum_{k'=1}^{d}[y]_{k'}/d$.

The embedding is then updated via two interaction layers. At each interaction layer l, the embedding is projected to two lower-dimensional spaces r_i,s_i via a learnable affine transform:

$$r_i^{(l)} = W_r^{(l)} x_i^{(l-1)} + b_r^{(l)} \tag{8}$$

$$s_i^{(l)} = W_s^{(l)} x_i^{(l-1)} + b_s^{(l)} \tag{9}$$

The r_i vector is used to retain information from the previous layer while the s_j vectors of neighbouring atoms will be used as messages and combined with geometric resources.

In the first layer, we only consider atoms within a short-range cutoff radius $R_c^{(\text{sr})} = 3.5$ Å. Short-range radial resources are obtained as:

$$g_{rad,i}^{(l)} = \sum_{j \in \mathcal{N}_{\text{sr}}(i)} s_j^{(l)} \otimes B(r_{ij}) f_c(r_{ij}) \tag{10}$$

where $\mathcal{N}_{\text{sr}}(i)$ is the ensemble of atoms located at a distance shorter than $R_c^{(\text{sr})}$, r_{ij} is the distance between atoms i and j, f_c is an envelope function going smoothly to zero at $R_c^{(\text{sr})}$, $\otimes$ represents the outer product between two vectors and $B(r_{ij})$ is a radial basis encoding the distance to a multidimensional vector. Here, we use the basis of Bessel functions proposed in ref. 50.

Angular resources are obtained by combining information from triplets of atoms. We start by forming a reduced chemical-radial basis D_{ij} and D_{ik} for the two edges forming the triplet:

$$\left[D_{ij}^{(l)}\right]_c = f_c(r_{ij}) \sum_{ab} \left[B(r_{ij})\right]_a \left[s_j^{(l)}\right]_b \left[W_{\text{ang}}^{(l)}\right]_{abc} \tag{11}$$

for all $j \in \mathcal{N}_{\text{sr}}(i)$. $W_{\text{ang}}^{(l)} \in \mathbb{R}^{\dim(B^{(a)}) \times \dim(s) \times d_a}$ is a trainable tensor and d_a a hyperparameter of the model. We then expand the angle between the two edges using a short Fourier expansion $[\Theta_{ijk}]_n = \cos(n\theta_{ijk})$ and combine the information as:

$$g_{ang,i}^{(l)} = (1 - \delta_{Z_i}^1) \cdot \sum_{\{jk\}} \Theta_{ijk} \otimes \left(D_{ij}^{(l)} \odot D_{ik}^{(l)}\right) \tag{12}$$

where $\odot$ represents element-wise multiplication. The term $(1 - \delta_{Z_i}^1)$ means that we neglect all triplets of atoms centered on Hydrogen atoms. This optimization provides a significant boost in performance, in particular when simulating molecules solvated in water. Hydrogen atoms thus only compute radial resources but their embeddings are still sensitive to angular information thanks to message-passing.

In the second interaction layer, we also build long-range messages using a shifted-force damped coulomb kernel[44] as a minimal radial basis:

$$[B^{(\text{lr})}(r_{ij})]_\lambda = \frac{1}{\sqrt{r_{ij}^2 + a_\lambda^2}^{\lambda+1}} - \frac{1}{\sqrt{{R_c^{(\text{lr})}}^2 + a_\lambda^2}^{\lambda+1}} + \frac{(\lambda+1) R_c^{(\text{lr})}(r_{ij} - R_c^{(\text{lr})})}{\sqrt{{R_c^{(\text{lr})}}^2 + a_\lambda^2}^{\lambda+3}} \tag{13}$$

for all j within the long-range cutoff radius $R_c^{(\text{lr})} = 7.5$Å. This minimal basis goes smoothly to zero at the cutoff radius for all λ and mimics the behaviour of screened charge-charge coulomb interactions for $\lambda = 0$. The trainable parameters a_λ (all initialized to 1Å) damp the interaction at short ranges to avoid divergences. The $\lambda = 0$

term is used as a descriptor for generalized charge-charge interactions as:

$$g_{q-q,i} = \sum_j [B^{(\mathrm{lr})}(r_{ij})]_0 W_{q-q} x_j^{(1)} \tag{14}$$

with $W_{q-q} \in \mathbb{R}^{d_{\mathrm{lr}} \times N_f}$ a matrix of trainable weights. We also include charge-dipole messages as:

$$g_{q-\mu,i} = \vec{\mu}_i \cdot \sum_j \frac{\vec{\mathbf{r}}_{ij}}{r_{ij}} [B^{(\mathrm{lr})}(r_{ij})]_1 W_{q-\mu} x_j^{(1)} \tag{15}$$

with $\vec{\mu}_i \in \mathbb{R}^{d_{\mathrm{lr}} \times 3}$ the "dipoles" located on atom i obtained as:

$$\vec{\mu}_i = \sum_{j \in \mathcal{N}_{\mathrm{sr}}(i)} \frac{\vec{\mathbf{r}}_{ij}}{r_{ij}} W_\mu g_{rad,ij}^{(2)} \tag{16}$$

At the end of each layer, the resources are mixed via a multi-layer perceptron MLP_l to form the embedding update:

$$\Delta x_i^{(l)} = MLP_l^{G(Z_i)}(r_i^{(l)} \mid\mid g_i^{(l)}) \tag{17}$$

$$x_i^{(l)} = LN\Big(\sigma(F^{(l)}) \odot x_i^{(l-1)} + \Delta x_i^{(l)}\Big) \tag{18}$$

with $F^{(l)} \in \mathbb{R}^{N_f}$ and $\sigma(F^{(l)})$ a trainable "forget gate" (with σ the sigmoid function). $g_i^{(l)}$ denotes the concatenation of all geometric resources:

$$g_i^{(1)} = g_{rad,i}^{(1)} \mid\mid g_{ang,i}^{(1)} \tag{19}$$

and

$$g_i^{(2)} = g_{rad,i}^{(2)} \mid\mid g_{ang,i}^{(2)} \mid\mid g_{q-q,i} \mid\mid g_{q-\mu,i} \tag{20}$$

B. Simulation Setup

All simulations have been performed using the GPU-accelerated Tinker-HP molecular dynamics software package[2,81] and leveraged its dedicated neural networks Deep-HP module[66] coupled to the FeNNol library[115]. FeNNix-Bio1 is presently functional on NVIDIA, AMD and Intel GPU computing platforms. All simulations used periodic boundary conditions with size of cubic boxes described in Supporting Information. Langevin dynamics was performed using the BAOAB integrator[83] and a 1fs timestep was employed in combination with a Berendsen[16] barostat.

C. Dataset and Training Configuration

1. Computational details

All conformations were computed using the ωB97M[93,105] DFT functional coupled to Grimme's D3(BJ)[54,55] dispersion correction, a strategy originally proposed in the original SPICE2 dataset to provide accurate and practicable computations[40,41]. However, following the exascale pipeline that we developed in reference [13], we combined the functional with the correlated consistent effective core potentials (ccECP)[152] and their companion aug-cc-pVTZ basis sets[152], as implemented in the PySCF package (and its GPU extension gpu4pyscf)[141–143]. The choice of the present effective core potentials preserves accuracy while increasing the computational efficiency compared to the explicit inclusion of core electrons. Moreover, this enables us to extend the dataset to metal ions (see next subsection) and to envision tractable future extension of the present DFT strategy to post Hartree-Fock methods where the use of valence-only calculations is crucial.

2. The Ocean dataset

The training set used to developed FeNNix-Bio1 is denoted Ocean. Its core component consists into an augmented SPICE2 dataset[40,41] that we introduced recently and denoted SPICE2(+)-ccECP. In the latter, 2,008,628 SPICE-2 initial configuration complementated by additional 100K conformations extracted from the ANI-2x dataset[35] were recomputed at the discussed effective core potentials/DFT level (see Computational Details). Note that the ANI-2X configurations were selected via a round of active learning using the uncertainty given by a preliminary version of the FeNNix-Bio-1. The present work goes further and the Ocean dataset includes also subset of under-represented but biologically relevant solvated ions, which includes Br, Ca, Cl, F, I, K, Li, Mg, Na and Zn. We adopted the SPICE2 protocol for solvated PubChem molecules[41] and modified it in order to take snapshots every 1 ps of the MD simulations with pre-selected number of the closest water molecules. For each ion, a 200 ps MD run was performed four times with either 2, 4, 6, or 8 closest water molecules being selected, thus generating 800 conformations per ion. Additionally, 2000 conformations solvated with 10 water molecules were produced by a 2000 ps MD simulation, with the goal to emphasize the largest water clusters. Overall, the solvated ions subset contains 28K conformations in total, with 2800 conformations per ionic species.

We then added synthetic data for isolated atoms so that the model predicts correct dissociation limits. Contrary to previous works that enforce the dissociation limit via the functional form of the potential[78,79,116], we chose to impose it in a data-driven way as we found that it improved the learning dynamics, in particular helping to better separate the scales of intra- and inter-molecular interactions. Finally, we added data for the isolated water molecule in very distorted geometries (up to the dissociation limit for one or both hydrogen atoms) using the Partridge-Schwenke model[111] that we slightly adjusted to reproduce the formation energy of the water molecule given by our chosen DFT functional.

From all these conformations, we filtered out the ones with absolute force components greater than 300 kcal/mol/Å. In total, our Ocean dataset comprises about 2,230,000 conformations among which we left 10% aside for validation and the remaining conformations for training. A key aspect of the Ocean dataset is that it is always growing due to finetuning processes and is evolving as the foundation model expands over chemical space.

3. Model training

The model was trained to reproduce formation energies (total DFT energy minus energy of isolated neutral atoms), forces as well as "internal energies" which are given by the difference in energy between a conformer and the minimum energy conformer of the same molecule in the dataset. We found that training the model on these internal energies enables it to better capture subtle energy differences in conformational changes, such as torsion energy profiles. The full loss function for our model is provided in eq. (21):

$$\begin{aligned}\mathcal{L}(\Theta; X, E, F, E_0, X_0) &= \lambda_E CRPS(E_{\text{ens}}(X,\Theta), E) \\ &+ \lambda_{E_0} CRPS(E_{\text{ens}}(X,\Theta) - E_{\text{ens}}(X_0,\Theta), E - E_0) \\ &+ \lambda_F MSE(-\nabla_X E_{\text{tot}}(X,\Theta), F) \\ &+ \lambda_{\tilde{E}} CRPS(\tilde{E}_{\text{ens}}(X,\Theta), E) \\ &+ \lambda_{\tilde{E}_0} CRPS(\tilde{E}_{\text{ens}}(X,\Theta) - \tilde{E}_{\text{ens}}(X_0,\Theta), E - E_0) \\ &+ \lambda_{\text{ZBL}} MSE(\Theta_{\text{ZBL}} - \Theta^{(0)}_{\text{ZBL}}) \end{aligned} \quad (21)$$

where Θ is the collection of trainable parameters of the model, X is a conformation sampled from the dataset, E is its DFT formation energy, F the DFT forces, X_0 the minimum energy conformation for the molecule sampled and E_0 its formation energy. $E_{\text{ens}}(X,\Theta)$ corresponds to the ensemble of energies outputted by the model and $E_{\text{tot}}(X,\Theta) = \sum_{j=1}^{N_{ens}} [E_{\text{ens}}(X,\Theta)]_j / N_{ens}$. The function $\tilde{E}_{\text{ens}}(X,\Theta)$ is a secondary energy model that is obtained as in equation (1) using an independent multilayer perceptron that is fed with the same embedding as for $E_{\text{ens}}(X,\Theta)$ (i.e. a secondary energy "head"). This secondary model is trained to reproduce energies only (i.e. no force information) and is intended as a second source of uncertainty quantification. The function MSE is the mean squared error loss function and $CRPS$ is the continuously ranked probability score for a normal distribution that is proposed in ref.[74] as a loss function for shallow ensemble models. The last term in equation (21) is a regularization for the parameters of the ZBL repulsion so that they don't deviate too much from the original parameters of ref.[170].

With energies in eV and distances in Å, the component weights are $\lambda_E = \lambda_{E_0} = \lambda_{\tilde{E}} = \lambda_{\tilde{E}_0} = 10$, $\lambda_F = 1000$ and $\lambda_{\text{ZBL}} = 10$.

The model was trained for 2,200,000 steps of AdaBelief optimizer[169] (as implemented in Optax[33]) with a batch size of 128 conformations sampled randomly from the training set. The learning rate is maintained fixed at 2e-4 for 500,000 steps and then decayed with a cosine scheduler to reach 1e-7 at step 2,000,000. It is then maintained fixed until the end of the training. We apply a weight decay of 1e-3 to all the parameters of the multilayer perceptrons, to the parameters of the affine transformations and to the $W^{(l)}_{\text{ang}}$ tensors. The actual model parameters are obtained via an exponential moving average of the parameters obtained at each step of the training run, with a decay parameter of 0.99. The training of FeNNix-Bio1 took approximately 30 hours on a single NVIDIA RTX3090 GPU using the FeNNol library[115].

After training, the model achieves a mean absolute error on the validation set of 0.6 kcal/mol (0.023 kcal/-mol/atom) for energies and 0.7 kcal/mol/Å for forces.

D. Validation of Uncertainty Quantification

Uncertainty quantification is particularly critical for foundation models as they are expected to be applied outside of their training data distribution. FeNNix-Bio1 quantifies uncertainties via the Direct Propagation of Shallow Ensembles (DPOSE) method proposed by Kellner and Ceriotti in ref.[74]. They showed that DPOSE provides well-calibrated and computationally inexpensive uncertainty estimates.

More precisely, FeNNix-Bio1 predicts two estimates of energy distributions, one trained targetting energies and forces – denoted E_{ens} – and one targeting energies only – denoted $\tilde{E}_{\text{ens}}$. From these two distributions, one can define multiple uncertainty estimators. The most straightforward ones simply use the standard deviations σ_0 and $\tilde{\sigma}_0$ independently. One can also combine information from the two distributions as:

$$\sigma_1^2 = \left(\sigma_0^2 + \tilde{\sigma}_0^2 + (\mu - \tilde{\mu})^2\right)/2 \quad (22)$$

where μ and $\tilde{\mu}$ denote the ensemble averages. We quantify the calibration of an uncertainty estimate σ by computing the scaling factor α such that $\alpha\sigma$ minimizes the Gaussian negative log-likelihood over the validation set $\alpha = \sqrt{\langle \epsilon^2/\sigma^2 \rangle_{\text{val}}}$ with ϵ the energy error with respect to DFT. A calibration of 1 thus indicates perfectly calibrated uncertainties in average. The calibration factors for σ_0, $\tilde{\sigma}_0$ and σ_1 are $\alpha_0 = 1.03$, $\tilde{\alpha}_0 = 1.20$ and $\alpha_1 = 0.99$ indicating a good calibration for all estimates, with a slight improvement with the combined estimator. We also quantify how informative the uncertainty estimates are by computing the Relative Log-Likelihood (RLL, see eq.(7) from ref.[74]) of the uncertainty estimates, respectively giving $RLL_0 = 43\%$, $\tilde{RLL}_0 = 42\%$ and $RLL_1 = 47\%$, in line with numerical experiments from ref.[74] on molecular datasets. These metrics thus indicate that the combined uncertainty estimator σ_1 should be slightly more reliable than the individual ensemble uncertainties.

Figure 9 shows the correlation between the σ_1 predicted uncertainty and the actual unsigned error compared to DFT energies for conformations from the validation set. A visual inspection and comparison to quantiles of an ideal Gaussian distribution of the errors reveal that uncertainty estimates are indeed well calibrated and informative.

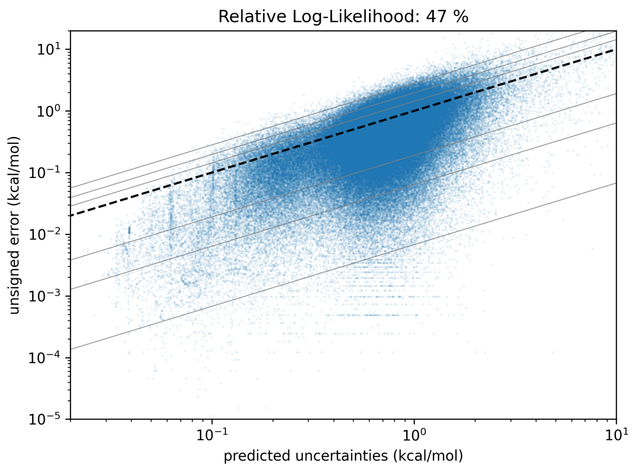

FIG. 9. Predicted uncertainty versus unsigned error for FeNNix-Bio1 over the validation set. The grey lines indicate, from bottom to top, the 0.5%, 5%, 15%, 85%, 95%, 99.5% quantiles for an ideal Gaussian distribution of the errors.

E. Alchemical Free Energy Calculations

For computing absolute binding or solvation free energies, we use the alchemical methods: to compute the free energy difference between two thermodynamical states A and B (for example A is the solvated molecule and B the gas-phase when computing the solvation free energy) we parameterize the hamiltonian of the system with a parameter λ so that for $\lambda = 1$ the system is in state A and for $\lambda = 0$, the system is in state B. Intermediate values correspond to potentially unphysical states that interpolate between the two physical states of interest.

In conventional force fields, one usually smoothly turns off intermolecular interactions by scaling them with a power of λ. Here, we achieve the decoupling by scaling all the pairwise cutoff functions $f_c(r_{ij})$ (that ensure a smooth spatial decoupling of the atoms when they leave each other's neighborhood) between atoms that should be decoupled by a function of λ, similarly to what was proposed in ref.[103]. As noted in ref.[103], a direct scaling of the interaction can lead to divergences when the nearly decoupled atoms get to close to each other. This is a well known property of alchemical simulations that led to the development of "soft-core potential" for conventional force fields[17]. In ref.[103], they simulate a soft-core potential with a ML model by adding λ as an input variable to the model and training it from scratch with additional synthetic dimer interactions that have been smoothed at short distances.

In this work, we chose to take advantage of the explicit repulsion in the model's functional form and to employ a solution that is closer to traditional methods and does not require synthetic data. We split the λ path in two parts: for $\lambda \in [0.5, 1]$, we scale the cutoff functions from 1 at $\lambda = 0$ to 0 at $\lambda = 1$, except for the explicit repulsion term; for $\lambda \in [0, 0.5]$ we scale the repulsion term and apply a soft-core modification of the interatomic distances to avoid divergences. Our scheme is summed up in equations (23),(24),(25). We define sub-parameters λ_e and λ_v as in ref.[82]:

$$\begin{aligned} \forall\lambda \in [0,1], \quad \lambda_e &= (2\lambda - 1)\; 1_{\lambda>0.5} \\ \lambda_v &= 2\lambda\; 1_{\lambda<=0.5} + 1_{\lambda>0.5} \end{aligned} \tag{23}$$

where $1_{\lambda>0.5}$ and $1_{\lambda<=0.5}$ are indicating functions. For pairs of atoms i,j that should be decoupled, we replace the cutoff functions by:

$$\tilde{f}_c(r_{ij}, \lambda_e, \lambda_v) = f_c(r_{ij}) \times (1 - \cos(\pi\lambda_e))/2 \tag{24}$$

and the ZBL repulsion by:

$$\begin{aligned} \tilde{E}_{\mathrm{ZBL}}(r_{ij}, \lambda_e, \lambda_v) = E_{\mathrm{ZBL}}\left(\sqrt{r_{ij}^2 + \alpha^2(1 - \lambda_v)}\right) \\ \times (1 - \cos(\pi\lambda_v))^2/4 \end{aligned} \tag{25}$$

with $\alpha = 0.5$Å the parameter controlling the smoothness of the soft-core. Finally, we linearly interpolate as a function of λ_e the charge embeddings e_{Q_i} of equation (5) using the charges explicitly computed in both end states (as this calculation only depends on the species composition of the system and the total charges of each states, this interpolation does not add significant calculation burden).

Keeping the full repulsion until the ML interactions are fully annihilated allows to avoid unphysical close contacts of atoms that are not present in the training set and that might otherwise product instabilities in the ML model. Our scheme thus allows for a smooth transition between states which is beneficial for any alchemical free energy calculation method and in particular for the Lambda-ABF scheme[82] that we employ in this work.

Note that the same smoothing effect could be realized in any ML model without explicit repulsion by smoothly adding a repulsion term for $\lambda \in [0.5, 1]$ while annihilating the ML interactions and then making it disappear as in eq. (25) for $\lambda \in [0, 0.5]$.

CODE AVAILABILITY

All calculations were performed using the FeNNol library (`https://github.com/thomasple/FeNNol`) and the Tinker-HP software (`https://github.com/TinkerTools/tinker-hp`).

DATA AVAILABILITY

Pretrained models are available on Github at `https://github.com/thomasple/FeNNol-PMC`

COMPETING INTERESTS

LL and JPP are shareholders and co-founders of Qubit Pharmaceuticals. All the remaining authors declare no conflict of interest.

AUTHOR CONTRIBUTION

Designed research: T. P., L. L., J.-P. P. ; **Performed simulations:** T. P., O.A., L. L. ; **Performed database computations:** A. B., E. P., C. V.; **Contributed analytic tools:** T. P., O.A, L. L., J.-P. P.; **Analyzed data:** T. P., L. L., J.-P. P.; **Wrote the paper:** T. P., L. L., J.-P. P. with the input of all authors.

ACKNOWLEDGMENT

This work was made possible thanks to funding from the European Research Council (ERC) under the European Union's Horizon 2020 research and innovation program (grant agreement No 810367), project EMC2 (JPP). We acknowledge EuroHPC Joint Undertaking for awarding the project IDs EHPC-DEV-2024D07-044 (E. P.) and EHPC-AI-2024A04-085 (E. P.) access to Leonardo at CINECA, Italy for DFT computations. An award for computer time was provided by the U.S. Department of Energy's (DOE) Innovative and Novel Computational Impact on Theory and Experiment (INCITE) Program (AB, JPP) on the Aurora Exascale supercomputer. This research used resources from the Argonne Leadership Computing Facility, a U.S. DOE Office of Science user facility at Argonne National Laboratory, which is supported by the Office of Science of the U.S. DOE under Contract No. DE-AC02-06CH11357. It was specifically to perform larger DFT computations with a number of electrons per molecules higher than 175. The learning of the FeNNix-Bio1 model and all molecular dynamics simulations were performed at IDRIS, GENCI (Jean Zay machine, France) on grants No. A0150712052 (J.-P.P.) and grant GC010815453 (Grand Challenge H100 Jean Zay, J.-P.P.).

[1] Jose LF Abascal and Carlos Vega. A general purpose model for the condensed phases of water: Tip4p/2005. *The Journal of chemical physics*, 123(23), 2005.

[2] Olivier Adjoua, Louis Lagardère, Luc-Henri Jolly, Arnaud Durocher, Thibaut Very, Isabelle Dupays, Zhi Wang, Théo Jaffrelot Inizan, Frédéric Célerse, Pengyu Ren, Jay W. Ponder, and Jean-Philip Piquemal. Tinker-hp: Accelerating molecular dynamics simulations of large complex systems with advanced point dipole polarizable force fields using gpus and multi-gpu systems. *Journal of Chemical Theory and Computation*, 17(4):2034–2053, 2021.

[3] Berni J Alder and Thomas Everett Wainwright. Studies in molecular dynamics. i. general method. *The Journal of Chemical Physics*, 31(2):459–466, 1959.

[4] Narjes Ansari, Francis Jing, Antoine Gagelin, Florent Hédin, Félix Aviat, Jérôme Hénin, Jean-Philip Piquemal, and Louis Lagardère. Lambda-abf-opes: Faster convergence with high accuracy in alchemical free energy calculations. *arXiv preprint arXiv:2502.17233*, 2025.

[5] Dylan Anstine, Roman Zubatyuk, and Olexandr Isayev. Aimnet2: a neural network potential to meet your neutral, charged, organic, and elemental-organic needs. *in proceedings*, 2024.

[6] Nongnuch Artrith, Tobias Morawietz, and Jörg Behler. High-dimensional neural-network potentials for multicomponent systems: Applications to zinc oxide. *Physical Review B*, 83(15):153101, 2011.

[7] Shalini Awasthi, Venkat Kapil, and Nisanth N Nair. Sampling free energy surfaces as slices by combining umbrella sampling and metadynamics. *Journal of Computational Chemistry*, 37(16):1413–1424, 2016.

[8] Minkyung Baek, Frank DiMaio, Ivan Anishchenko, Justas Dauparas, Sergey Ovchinnikov, Gyu Rie Lee, Jue Wang, Qian Cong, Lisa N Kinch, R Dustin Schaeffer, et al. Accurate prediction of protein structures and interactions using a three-track neural network. *Science*, 373(6557):871–876, 2021.

[9] Albert P Bartók, Mike C Payne, Risi Kondor, and Gábor Csányi. Gaussian approximation potentials: The accuracy of quantum mechanics, without the electrons. *Physical Review Letters*, 104(13):136403, 2010.

[10] Ilyes Batatia, Philipp Benner, Yuan Chiang, Alin M. Elena, DÃąvid P. KovÃącs, Janosh Riebesell, Xavier R. Advincula, Mark Asta, Matthew Avaylon, William J. Baldwin, Fabian Berger, Noam Bernstein, Arghya Bhowmik, Samuel M. Blau, Vlad CÄČrare, James P. Darby, Sandip De, Flaviano Della Pia, Volker L. Deringer, Rokas ElijoÅąius, Zakariya El-Machachi, Fabio Falcioni, Edvin Fako, Andrea C. Ferrari, Annalena Genreith-Schriever, Janine George, Rhys E. A. Goodall, Clare P. Grey, Petr Grigorev, Shuang Han, Will Handley, Hendrik H. Heenen, Kersti Hermansson, Christian Holm, Jad Jaafar, Stephan Hofmann, Konstantin S. Jakob, Hyunwook Jung, Venkat Kapil, Aaron D. Kaplan, Nima Karimitari, James R. Kermode, Namu Kroupa, Jolla Kullgren, Matthew C. Kuner, Domantas Kuryla, Guoda Liepuoniute, Johannes T. Margraf, Ioan-Bogdan Magdau, Angelos Michaelides, J. Harry Moore, Aakash A. Naik, Samuel P. Niblett, Sam Walton Norwood, Niamh O'Neill, Christoph Ortner, Kristin A. Persson, Karsten Reuter, Andrew S. Rosen, Lars L. Schaaf, Christoph Schran, Benjamin X. Shi, Eric Sivonxay, TamÃąs K. Stenczel, Viktor Svahn, Christopher Sutton, Thomas D. Swinburne, Jules Tilly, Cas van der Oord, Eszter Varga-Umbrich, Tejs Vegge, Martin Vondrák, Yangshuai Wang, William C. Witt, Fabian Zills, and GÃąbor Csányi. A foundation model for atomistic materials chemistry, 2024.

[11] Simon Batzner, Albert Musaelian, Lixin Sun, Mario Geiger, Jonathan P Mailoa, Mordechai Kornbluth, Nicola Molinari, Tess E Smidt, and Boris Kozinsky. E(3)-equivariant graph neural networks for data-efficient and accurate interatomic potentials. *Nature Communications*, 13(1):1–11, 2022.

[12] Jörg Behler and Michele Parrinello. Generalized neural-network representation of high-dimensional potential-energy surfaces. *Physical Review Letters*, 98(14):146401, 2007.

[13] Anouar Benali, Thomas Plé, Olivier Adjoua, Thomas Applencourt, Raymond Clay III Marharyta Blazhynska, Kevin Gasperich, Khalid Hossain, Christopher Knight Jeongnim Kim, Jaron T. Krogel, Yvon Maday, Maxime Maria, Mathieu Montes, Ye Luo, Evgeny Posenitskiy, Corentin Villot, Venkat Vishwanath, Louis Lagardère, and Jean-Philip Piquemal. Pushing the accuracy limit of foundation neural network models with quantum monte carlo forces and path integrals, 2025.

[14]Herman JC Berendsen, J Raul Grigera, and Tjerk P Straatsma. The missing term in effective pair potentials. *Journal of Physical Chemistry*, 91(24):6269–6271, 1987.

[15]Herman JC Berendsen, James PM Postma, Wilfred F van Gunsteren, and Jan Hermans. Interaction models for water in relation to protein hydration. In *Intermolecular forces: proceedings of the fourteenth Jerusalem symposium on quantum chemistry and biochemistry held in jerusalem, israel, april 13–16, 1981*, pages 331–342. Springer, 1981.

[16]Herman JC Berendsen, JPM van Postma, Wilfred F Van Gunsteren, ARHJ DiNola, and Jan R Haak. Molecular dynamics with coupling to an external bath. *The Journal of Chemical Physics*, 81(8):3684–3690, 1984.

[17]Thomas C Beutler, Alan E Mark, René C van Schaik, Paul R Gerber, and Wilfred F Van Gunsteren. Avoiding singularities and numerical instabilities in free energy calculations based on molecular simulations. *Chemical physics letters*, 222(6):529–539, 1994.

[18]Filippo Bigi, Sergey N Pozdnyakov, and Michele Ceriotti. Wigner kernels: body-ordered equivariant machine learning without a basis. *arXiv preprint arXiv:2303.04124*, 2023.

[19]Camille Bilodeau, Wengong Jin, Tommi Jaakkola, Regina Barzilay, and Klavs F Jensen. Generative models for molecular discovery: Recent advances and challenges. *Wiley Interdisciplinary Reviews: Computational Molecular Science*, 12(5):e1608, 2022.

[20]Marharyta Blazhynska, Louis Lagardère, Chengwen Liu, Olivier Adjoua, Pengyu Ren, and Jean-Philip Piquemal. Water–glycan interactions drive the sars-cov-2 spike dynamics: insights into glycan-gate control and camouflage mechanisms. *Chemical Science*, 15(35):14177–14187, 2024.

[21]Rishi Bommasani, Drew A Hudson, Ehsan Adeli, Russ Altman, Simran Arora, Sydney von Arx, Michael S Bernstein, Jeannette Bohg, Antoine Bosselut, Emma Brunskill, et al. On the opportunities and risks of foundation models. *arXiv preprint arXiv:2108.07258*, 2021.

[22]Joel M Bowman, Chen Qu, Riccardo Conte, Apurba Nandi, Paul L Houston, and Qi Yu. δ-machine learned potential energy surfaces and force fields. *Journal of Chemical Theory and Computation*, 19(1):1–17, 2022.

[23]James Bradbury, Roy Frostig, Peter Hawkins, Matthew James Johnson, Chris Leary, Dougal Maclaurin, George Necula, Adam Paszke, Jake VanderPlas, Skye Wanderman-Milne, and Qiao Zhang. JAX: composable transformations of Python+NumPy programs, 2018.

[24]Christian J Burnham and Sotiris S Xantheas. Development of transferable interaction models for water. iii. reparametrization of an all-atom polarizable rigid model (ttm2–r) from first principles. *The Journal of Chemical Physics*, 116(4):1500–1510, 2002.

[25]Weilin Cai, Juyong Jiang, Fan Wang, Jing Tang, Sunghun Kim, and Jiayi Huang. A survey on mixture of experts. *arXiv preprint arXiv:2407.06204*, 2024.

[26]R. Car and M. Parrinello. Unified approach for molecular dynamics and density-functional theory. *Physical Review Letters*, 55:2471–2474, Nov 1985.

[27]David A Case, Tom A Darden, Thomas E Cheatham, Carlos L Simmerling, Junmei Wang, Robert E Duke, Ray Luo, MRCW Crowley, Ross C Walker, Wei Zhang, et al. Amber 10. *in proceedings*, 2008.

[28]Gong Chen, Théo Jaffrelot Inizan, Thomas Plé, Louis Lagardère, Jean-Philip Piquemal, and Yvon Maday. Advancing force fields parameterization: A directed graph attention networks approach. *Journal of Chemical Theory and Computation*, 20(13):5558–5569, 2024.

[29]Gong Chen, Théo Jaffrelot Inizan, Thomas Plé, Louis LagardÃÍre, Jean-Philip Piquemal, and Yvon Maday. Advancing force fields parameterization: A directed graph attention networks approach. *Journal of Chemical Theory and Computation*, 20(13):5558–5569, 2024. PMID: 38875012.

[30]Junmin Chen and Kuang Yu. Phyneo: A neural-network-enhanced physics-driven force field development workflow for bulk organic molecule and polymer simulations. *Journal of Chemical Theory and Computation*, 20(1):253–265, 2023.

[31]Stefan Chmiela, Huziel E Sauceda, Klaus-Robert Müller, and Alexandre Tkatchenko. Towards exact molecular dynamics simulations with machine-learned force fields. *Nature Communications*, 9(1):1–10, 2018.

[32]Gerardo Andrés Cisneros, Kjartan Thor Wikfeldt, Lars OjamÃďe, Jibao Lu, Yao Xu, Hedieh Torabifard, Albert P. BartÃşk, GÃąbor Csányi, Valeria Molinero, and Francesco Paesani. Modeling molecular interactions in water: From pairwise to many-body potential energy functions. *Chemical Reviews*, 116(13):7501–7528, 2016. PMID: 27186804.

[33]DeepMind, Igor Babuschkin, Kate Baumli, Alison Bell, Surya Bhupatiraju, Jake Bruce, Peter Buchlovsky, David Budden, Trevor Cai, Aidan Clark, Ivo Danihelka, Antoine Dedieu, Claudio Fantacci, Jonathan Godwin, Chris Jones, Ross Hemsley, Tom Hennigan, Matteo Hessel, Shaobo Hou, Steven Kapturowski, Thomas Keck, Iurii Kemaev, Michael King, Markus Kunesch, Lena Martens, Hamza Merzic, Vladimir Mikulik, Tamara Norman, George Papamakarios, John Quan, Roman Ring, Francisco Ruiz, Alvaro Sanchez, Laurent Sartran, Rosalia Schneider, Eren Sezener, Stephen Spencer, Srivatsan Srinivasan, Miloš Stanojević, Wojciech Stokowiec, Luyu Wang, Guangyao Zhou, and Fabio Viola. The DeepMind JAX Ecosystem, 2020.

[34]Yuqing Deng and Benoît Roux. Calculation of standard binding free energies: Aromatic molecules in the t4 lysozyme l99a mutant. *Journal of Chemical Theory and Computation*, 2(5):1255–1273, 2006.

[35]Christian Devereux, Justin S. Smith, Kate K. Huddleston, Kipton Barros, Roman Zubatyuk, Olexandr Isayev, and Adrian E. Roitberg. Extending the applicability of the ani deep learning molecular potential to sulfur and halogens. *Journal of Chemical Theory and Computation*, 16(7):4192–4202, 2020.

[36]Mike Devereux, Nohad Gresh, Jean-Philip Piquemal, and Markus Meuwly. A supervised fitting approach to force field parametrization with application to the sibfa polarizable force field. *Journal of Computational Chemistry*, 35(21):1577–1591, 2014.

[37]Serena Donnini, Alan E Mark, André H Juffer, and Alessandra Villa. Incorporating the effect of ionic strength in free energy calculations using explicit ions. *Journal of computational chemistry*, 26(2):115–122, 2005.

[38]Pavlo O Dral, Fuchun Ge, Yi-Fan Hou, Peikun Zheng, Yuxinxin Chen, Mario Barbatti, Olexandr Isayev, Cheng Wang, Bao-Xin Xue, Max Pinheiro Jr, et al. Mlatom 3: A platform for machine learning-enhanced computational chemistry simulations and workflows. *Journal of Chemical Theory and Computation*, 20(3):1193–1213, 2024.

[39]Robert E Duke, Oleg N Starovoytov, Jean-Philip Piquemal, and G Andrés Cisneros. Gem*: A molecular electronic density-based force field for molecular dynamics simulations. *Journal of Chemical Theory and Computation*, 10(4):1361–1365, 2014.

[40]Peter Eastman, Pavan Kumar Behara, David L Dotson, Raimondas Galvelis, John E Herr, Josh T Horton, Yuezhi Mao, John D Chodera, Benjamin P Pritchard, Yuanqing Wang, et al. Spice, a dataset of drug-like molecules and peptides for training machine learning potentials. *Scientific Data*, 10(1):11, 2023.

[41]Peter Eastman, Benjamin P. Pritchard, John D. Chodera, and Thomas E. Markland. Nutmeg and spice: Models and data for biomolecular machine learning. *Journal of Chemical Theory and Computation*, 20(19):8583–8593, 2024.

[42]Léa El Khoury, Frédéric Célerse, Louis Lagardère, Luc-Henri Jolly, Etienne Derat, Zeina Hobaika, Richard G Maroun, Pengyu Ren, Serge Bouaziz, Nohad Gresh, et al. Reconciling nmr structures of the hiv-1 nucleocapsid protein ncp7 using extensive polarizable force field free-energy simulations. *Journal of chemical theory and computation*, 16(4):2013–2020, 2020.

[43]George S Fanourgakis and Sotiris S Xantheas. Development of transferable interaction potentials for water. v. extension of the flexible, polarizable, thole-type model potential (TTM3-F,

v. 3.0) to describe the vibrational spectra of water clusters and liquid water. *The Journal of Chemical Physics*, 128(7):074506, 2008.

[44] Christopher J Fennell and J Daniel Gezelter. Is the ewald summation still necessary? pairwise alternatives to the accepted standard for long-range electrostatics. *The Journal of chemical physics*, 124(23), 2006.

[45] Giacomo Fiorin, Michael L Klein, and Jérôme Hénin. Using collective variables to drive molecular dynamics simulations. *Molecular Physics*, 111(22-23):3345–3362, 2013.

[46] Giacomo Fiorin, Fabrizio Marinelli, Lucy R Forrest, Haochuan Chen, Christophe Chipot, Axel Kohlmeyer, Hubert Santuz, and Jérôme Hénin. Expanded functionality and portability for the colvars library. *The Journal of Physical Chemistry B*, 128(45):11108–11123, 2024.

[47] Haohao Fu, Hong Zhang, Haochuan Chen, Xueguang Shao, Christophe Chipot, and Wensheng Cai. Zooming across the free-energy landscape: shaving barriers, and flooding valleys. *The journal of physical chemistry letters*, 9(16):4738–4745, 2018.

[48] Haohao Fu, Mengchen Zhou, Christophe Chipot, and Wensheng Cai. Overcoming sampling issues and improving computational efficiency in collective-variable-based enhanced-sampling simulations: A tutorial. *The Journal of Physical Chemistry B*, 128(40):9706–9713, 2024.

[49] Johannes Gasteiger, Florian Becker, and Stephan Günnemann. Gemnet: Universal directional graph neural networks for molecules. *Advances in Neural Information Processing Systems*, 34:6790–6802, 2021.

[50] Johannes Gasteiger, Janek Groß, and Stephan Günnemann. Directional message passing for molecular graphs. *arXiv preprint arXiv:2003.03123*, 2020.

[51] Ling Ge, Leonardo Bernasconi, and Patricia Hunt. Linking electronic and molecular structure: insight into aqueous chloride solvation. *Physical Chemistry Chemical Physics*, 15(31):13169–13183, 2013.

[52] Justin Gilmer, Samuel S Schoenholz, Patrick F Riley, Oriol Vinyals, and George E Dahl. Neural message passing for quantum chemistry. In *International conference on machine learning*, pages 1263–1272. PMLR, 2017.

[53] Nohad Gresh, G Andrés Cisneros, Thomas A Darden, and Jean-Philip Piquemal. Anisotropic, polarizable molecular mechanics studies of inter-and intramolecular interactions and ligand-macromolecule complexes. a bottom-up strategy. *Journal of Chemical Theory and Computation*, 3(6):1960–1986, 2007.

[54] Stefan Grimme, Jens Antony, Stephan Ehrlich, and Helge Krieg. A consistent and accurate ab initio parametrization of density functional dispersion correction (dft-d) for the 94 elements h-pu. *The Journal of Chemical Physics*, 132(15):154104, 04 2010.

[55] Stefan Grimme, Stephan Ehrlich, and Lars Goerigk. Effect of the damping function in dispersion corrected density functional theory. *Journal of Computational Chemistry*, 32(7):1456–1465, 2011.

[56] Andrea Grisafi and Michele Ceriotti. Incorporating long-range physics in atomic-scale machine learning. *The Journal of Chemical Physics*, 151(20):204105, 2019.

[57] Andrea Grisafi, Jigyasa Nigam, and Michele Ceriotti. Multi-scale approach for the prediction of atomic scale properties. *Chemical Science*, 12(6):2078–2090, 2021.

[58] Alan Grossfield, Pengyu Ren, and Jay W Ponder. Ion solvation thermodynamics from simulation with a polarizable force field. *Journal of the American Chemical Society*, 125(50):15671–15682, 2003.

[59] Leonardo Guidoni and Ursula Rothlisberger. Scanning reactive pathways with orbital biased molecular dynamics. *Journal of chemical theory and computation*, 1(4):554–560, 2005.

[60] Bertrand Guillot. A reappraisal of what we have learnt during three decades of computer simulations on water. *Journal of molecular liquids*, 101(1-3):219–260, 2002.

[61] Chris M Handley and Paul LA Popelier. Dynamically polarizable water potential based on multipole moments trained by machine learning. *Journal of chemical theory and computation*, 5(6):1474–1489, 2009.

[62] Hans W Horn, William C Swope, Jed W Pitera, Jeffry D Madura, Thomas J Dick, Greg L Hura, and Teresa Head-Gordon. Development of an improved four-site water model for biomolecular simulations: Tip4p-ew. *The Journal of Chemical Physics*, 120(20):9665–9678, 2004.

[63] Jürg Hutter and Marcella Iannuzzi. Cpmd: Car-parrinello molecular dynamics. *Zeitschrift für Kristallographie-Crystalline Materials*, 220(5-6):549–551, 2005.

[64] Marcella Iannuzzi, Alessandro Laio, and Michele Parrinello. Efficient exploration of reactive potential energy surfaces<? format?> using car-parrinello molecular dynamics. *Physical review letters*, 90(23):238302, 2003.

[65] Kevin Maik Jablonka, Philippe Schwaller, Andres Ortega-Guerrero, and Berend Smit. Leveraging large language models for predictive chemistry. *Nature Machine Intelligence*, 6(2):161–169, 2024.

[66] Théo Jaffrelot Inizan, Thomas Plé, Olivier Adjoua, Pengyu Ren, Hatice Gokcan, Olexandr Isayev, Louis Lagardère, and Jean-Philip Piquemal. Scalable hybrid deep neural networks/polarizable potentials biomolecular simulations including long-range effects. *Chemical Science*, 14:5438–5452, 2023.

[67] Zhifeng Jing, Chengwen Liu, Sara Y. Cheng, Rui Qi, Brandon D. Walker, Jean-Philip Piquemal, and Pengyu Ren. Polarizable force fields for biomolecular simulations: Recent advances and applications. *Ann. Rev. Biophys.*, 48(1):371–394, 2019.

[68] William L Jorgensen, Jayaraman Chandrasekhar, Jeffry D Madura, Roger W Impey, and Michael L Klein. Comparison of simple potential functions for simulating liquid water. *The Journal of chemical physics*, 79(2):926–935, 1983.

[69] William L. Jorgensen, David S. Maxwell, and Julian Tirado-Rives. Development and testing of the opls all-atom force field on conformational energetics and properties of organic liquids. *Journal of the American Chemical Society*, 118(45):11225–11236, 1996.

[70] John Jumper, Richard Evans, Alexander Pritzel, Tim Green, Michael Figurnov, Olaf Ronneberger, Kathryn Tunyasuvunakool, Russ Bates, Augustin Žídek, Anna Potapenko, et al. Highly accurate protein structure prediction with alphafold. *Nature*, 596(7873):583–589, 2021.

[71] Adil Kabylda, J Thorben Frank, Sergio Suarez Dou, Almaz Khabibrakhmanov, Leonardo Medrano Sandonas, Oliver T Unke, Stefan Chmiela, Klaus-Robert Müller, and Alexandre Tkatchenko. Molecular simulations with a pretrained neural network and universal pairwise force fields. *in proceedings*, 2025.

[72] Sachini P Kadaoluwa Pathirannahalage, Nastaran Meftahi, Aaron Elbourne, Alessia CG Weiss, Chris F McConville, Agilio Padua, David A Winkler, Margarida Costa Gomes, Tamar L Greaves, Tu C Le, et al. Systematic comparison of the structural and dynamic properties of commonly used water models for molecular dynamics simulations. *Journal of Chemical Information and Modeling*, 61(9):4521–4536, 2021.

[73] Amara Katabarwa, Katerina Gratsea, Athena Caesura, and Peter D Johnson. Early fault-tolerant quantum computing. *PRX quantum*, 5(2):020101, 2024.

[74] Matthias Kellner and Michele Ceriotti. Uncertainty quantification by direct propagation of shallow ensembles. *arXiv preprint arXiv:2402.16621*, 2024.

[75] Tsz Wai Ko, Jonas A Finkler, Stefan Goedecker, and Jörg Behler. A fourth-generation high-dimensional neural network potential with accurate electrostatics including non-local charge transfer. *Nature Communications*, 12(1):1–11, 2021.

[76] Emir Kocer, Tsz Wai Ko, and Jörg Behler. Neural network potentials: A concise overview of methods. *Annual review of physical chemistry*, 73:163–186, 2022.

[77] W. Kohn and L. J. Sham. Self-consistent equations including exchange and correlation effects. *Physical Review*, 140:A1133–A1138, Nov 1965.

[78] Dávid Péter Kovács, J Harry Moore, Nicholas J Browning, Ilyes Batatia, Joshua T Horton, Venkat Kapil, William C Witt, Ioan-Bogdan Magdău, Daniel J Cole, and Gábor Csányi. Mace-off23: Transferable machine learning force fields for organic molecules. *arXiv preprint arXiv:2312.15211*, 2023.

[79] Dávid Péter Kovács, Cas van der Oord, Jiri Kucera, Alice EA Allen, Daniel J Cole, Christoph Ortner, and Gábor Csányi. Linear atomic cluster expansion force fields for organic molecules: beyond rmse. *Journal of chemical theory and computation*, 17(12):7696–7711, 2021.

[80] Thomas D Kühne, Marcella Iannuzzi, Mauro Del Ben, Vladimir V Rybkin, Patrick Seewald, Frederick Stein, Teodoro Laino, Rustam Z Khaliullin, Ole Schütt, Florian Schiffmann, et al. Cp2k: An electronic structure and molecular dynamics software package-quickstep: Efficient and accurate electronic structure calculations. *The Journal of Chemical Physics*, 152(19), 2020.

[81] Louis Lagardère, Luc-Henri Jolly, Filippo Lipparini, FÃľlix Aviat, Benjamin Stamm, Zhifeng F. Jing, Matthew Harger, Hedieh Torabifard, G. AndrÃľs Cisneros, Michael J. Schnieders, Nohad Gresh, Yvon Maday, Pengyu Y. Ren, Jay W. Ponder, and Jean-Philip Piquemal. Tinker-hp: a massively parallel molecular dynamics package for multiscale simulations of large complex systems with advanced point dipole polarizable force fields. *Chemical Science*, 9:956–972, 2018.

[82] Louis Lagardère, Lise Maurin, Olivier Adjoua, Krystel El Hage, Pierre Monmarché, Jean-Philip Piquemal, and Jérôme Hénin. Lambda-abf: Simplified, portable, accurate, and cost-effective alchemical free-energy computation. *Journal of Chemical Theory and Computation*, 20(11):4481–4498, 2024.

[83] Benedict Leimkuhler and Charles Matthews. Rational construction of stochastic numerical methods for molecular sampling. *Applied Mathematics Research eXpress*, 2013(1):34–56, 2013.

[84] Itai Leven, Hongxia Hao, Songchen Tan, Xingyi Guan, Katheryn A. Penrod, Dooman Akbarian, Benjamin Evangelisti, Md Jamil Hossain, Md Mahbubul Islam, Jason P. Koski, Stan Moore, Hasan Metin Aktulga, Adri C. T. van Duin, and Teresa Head-Gordon. Recent advances for improving the accuracy, transferability, and efficiency of reactive force fields. *Journal of Chemical Theory and Computation*, 17(6):3237–3251, 2021.

[85] Kresten Lindorff-Larsen, Stefano Piana, Ron O Dror, and David E Shaw. How fast-folding proteins fold. *Science*, 334(6055):517–520, 2011.

[86] Chengwen Liu, Jean-Philip Piquemal, and Pengyu Ren. Amoeba+ classical potential for modeling molecular interactions. *Journal of Chemical Theory and Computation*, 15(7):4122–4139, 2019.

[87] Chengwen Liu, Jean-Philip Piquemal, and Pengyu Ren. Amoeba+ classical potential for modeling molecular interactions. *Journal of Chemical Theory and Computation*, 15(7):4122–4139, 2019.

[88] Chengwen Liu, Jean-Philip Piquemal, and Pengyu Ren. Implementation of geometry-dependent charge flux into the polarizable amoeba+ potential. *The journal of physical chemistry letters*, 11(2):419–426, 2019.

[89] Chengwen Liu, Jean-Philip Piquemal, and Pengyu Ren. Implementation of geometry-dependent charge flux into the polarizable amoeba+ potential. *The Journal of Physical Chemistry Letters*, 11(2):419–426, 2020.

[90] Nicholas Lubbers, Justin S Smith, and Kipton Barros. Hierarchical modeling of molecular energies using a deep neural network. *The Journal of Chemical Physics*, 148(24), 2018.

[91] Alexander D. MacKerell. Chapter 7 empirical force fields for proteins: Current status and future directions, 2005.

[92] Etienne Mangaud, Simon Huppert, Thomas Plé, Philippe Depondt, Sara Bonella, and Fabio Finocchi. The fluctuation–dissipation theorem as a diagnosis and cure for zero-point energy leakage in quantum thermal bath simulations. *Journal of Chemical Theory and Computation*, 15(5):2863–2880, 2019.

[93] Narbe Mardirossian and Martin Head-Gordon. ĪĽb97m-v: A combinatorially optimized, range-separated hybrid, meta-gga density functional with vv10 nonlocal correlation. *The Journal of Chemical Physics*, 144(21):214110, 06 2016.

[94] Pekka Mark and Lennart Nilsson. Structure and dynamics of the tip3p, spc, and spc/e water models at 298 k. *The Journal of Physical Chemistry A*, 105(43):9954–9960, 2001.

[95] Dominik Marx and Jürg Hutter. *Ab initio molecular dynamics: basic theory and advanced methods*. Cambridge University Press, 2009.

[96] Nastasia Mauger, Thomas Plé, Louis Lagardère, Sara Bonella, Étienne Mangaud, Jean-Philip Piquemal, and Simon Huppert. Nuclear quantum effects in liquid water at near classical computational cost using the adaptive quantum thermal bath. *The Journal of Physical Chemistry Letters*, 12(34):8285–8291, 2021.

[97] Nastasia Mauger, Thomas Plé, Louis Lagardère, Simon Huppert, and Jean-Philip Piquemal. Improving condensed-phase water dynamics with explicit nuclear quantum effects: The polarizable q-amoeba force field. *The Journal of Physical Chemistry B*, 126(43):8813–8826, 2022.

[98] Nastasia Mauger, Thomas Plé, Louis Lagardère, Simon Huppert, and Jean-Philip Piquemal. The q-amoeba (cf) polarizable potential. *arXiv preprint arXiv:2502.12708*, 2025.

[99] Nastasia Mauger, Thomas Plé, Louis LagardÃÍre, Simon Huppert, and Jean-Philip Piquemal. Improving condensed-phase water dynamics with explicit nuclear quantum effects: The polarizable q-amoeba force field. *The Journal of Physical Chemistry B*, 126(43):8813–8826, 2022.

[100] J Andrew McCammon, Bruce R Gelin, and Martin Karplus. Dynamics of folded proteins. *Nature*, 267(5612):585–590, 1977.

[101] Josef Melcr and Jean-Philip Piquemal. Accurate biomolecular simulations account for electronic polarization. *Frontiers in Molecular Biosciences*, 6:143, 2019.

[102] Matthew Merski and Brian K Shoichet. The impact of introducing a histidine into an apolar cavity site on docking and ligand recognition. *Journal of medicinal chemistry*, 56(7):2874–2884, 2013.

[103] J Harry Moore, Daniel J Cole, and Gabor Csanyi. Computing hydration free energies of small molecules with first principles accuracy. *arXiv preprint arXiv:2405.18171*, 2024.

[104] Albert Musaelian, Simon Batzner, Anders Johansson, Lixin Sun, Cameron J Owen, Mordechai Kornbluth, and Boris Kozinsky. Learning local equivariant representations for large-scale atomistic dynamics. *Nature Communications*, 14(1):579, 2023.

[105] Asim Najibi and Lars Goerigk. The nonlocal kernel in van der waals density functionals as an additive correction: An extensive analysis with special emphasis on the b97m-v and ωb97m-v approaches. *Journal of Chemical Theory and Computation*, 14(11):5725–5738, 2018.

[106] Yiling Nan, Prabin Baral, Asuka A. Orr, Haley M. Michel, Justin A. Lemkul, and Alexander D. Jr. MacKerell. Balancing group 1 monoatomic ionâĂŞpolar compound interactions in the polarizable drude force field: Application in protein and nucleic acid systems. *The Journal of Physical Chemistry B*, 128(49):12078–12091, 2024.

[107] Sehr Naseem-Khan, Nohad Gresh, Alston J. Misquitta, and Jean-Philip Piquemal. Assessment of sapt and supermolecular eda approaches for the development of separable and polarizable force fields. *Journal of Chemical Theory and Computation*, 17(5):2759–2774, 2021.

[108] Sehr Naseem-Khan, Louis Lagardère, Christophe Narth, G Andrés Cisneros, Pengyu Ren, Nohad Gresh, and Jean-Philip Piquemal. Development of the quantum-inspired sibfa many-body polarizable force field: enabling condensed-phase molecular dynamics simulations. *Journal of Chemical Theory and Computation*, 18(6):3607–3621, 2022.

[109] Grzegorz Nawrocki, Igor Leontyev, Serzhan Sakipov, Mikhail Darkhovskiy, Igor Kurnikov, Leonid Pereyaslavets, Ganesh Kamath, Ekaterina Voronina, Oleg Butin, Alexey Illarionov, et al. Protein–ligand binding free-energy calculations with arrowâŤĂ

a purely first-principles parameterized polarizable force field. *Journal of Chemical Theory and Computation*, 18(12):7751–7763, 2022.

[110] Etienne Palos, Eleftherios Lambros, Steven Swee, Jie Hu, Saswata Dasgupta, and Francesco Paesani. Assessing the interplay between functional-driven and density-driven errors in dft models of water. *Journal of Chemical Theory and Computation*, 18(6):3410–3426, 2022.

[111] Harry Partridge and David W Schwenke. The determination of an accurate isotope dependent potential energy surface for water from extensive ab initio calculations and experimental data. *The Journal of Chemical Physics*, 106(11):4618–4639, 1997.

[112] Leonid Pereyaslavets, Igor Kurnikov, Ganesh Kamath, Oleg Butin, Alexey Illarionov, Igor Leontyev, Michael Olevanov, Michael Levitt, Roger D Kornberg, and Boris Fain. On the importance of accounting for nuclear quantum effects in ab initio calibrated force fields in biological simulations. *Proceedings of the National Academy of Sciences*, 115(36):8878–8882, 2018.

[113] James C Phillips, Rosemary Braun, Wei Wang, James Gumbart, Emad Tajkhorshid, Elizabeth Villa, Christophe Chipot, Robert D Skeel, Laxmikant Kale, and Klaus Schulten. Scalable molecular dynamics with namd. *Journal of Computational Chemistry*, 26(16):1781–1802, 2005.

[114] Max Pinheiro, Fuchun Ge, Nicolas Ferré, Pavlo O Dral, and Mario Barbatti. Choosing the right molecular machine learning potential. *Chemical Science*, 12(43):14396–14413, 2021.

[115] Thomas Plé, Olivier Adjoua, Louis Lagardère, and Jean-Philip Piquemal. FeNNol: An efficient and flexible library for building force-field-enhanced neural network potentials. *The Journal of Chemical Physics*, 161(4):042502, 07 2024.

[116] Thomas Plé, Louis Lagardère, and Jean-Philip Piquemal. Force-field-enhanced neural network interactions: from local equivariant embedding to atom-in-molecule properties and long-range effects. *Chemical Science*, 14:12554–12569, 2023.

[117] Thomas Plé, Nastasia Mauger, Olivier Adjoua, Théo Jaffrelot Inizan, Louis Lagardère, Simon Huppert, and Jean-Philip Piquemal. Routine molecular dynamics simulations including nuclear quantum effects: from force fields to machine learning potentials. *Journal of Chemical Theory and Computation*, 19(5):1432–1445, 2023.

[118] Jay W Ponder, Chuanjie Wu, Pengyu Ren, Vijay S Pande, John D Chodera, Michael J Schnieders, Imran Haque, David L Mobley, Daniel S Lambrecht, Robert A DiStasio Jr, et al. Current status of the amoeba polarizable force field. *The Journal of Physical Chemistry B*, 114(8):2549–2564, 2010.

[119] Zhuoran Qiao, Anders S Christensen, Matthew Welborn, Frederick R Manby, Anima Anandkumar, and Thomas F Miller III. Unite: Unitary n-body tensor equivariant network with applications to quantum chemistry. *arXiv preprint arXiv:2105.14655*, 2021.

[120] Chen Qu, Qi Yu, Paul L Houston, Riccardo Conte, Apurba Nandi, and Joel M Bowman. Interfacing q-aqua with a polarizable force field: The best of both worlds. *Journal of Chemical Theory and Computation*, 2023.

[121] Kavindri Ranasinghe, Adam L Baskerville, Geoffrey PF Wood, and Gerhard Koenig. Basic stability tests of machine learning potentials for molecular simulations in computational drug discovery. *arXiv preprint arXiv:2503.11537*, 2025.

[122] Sandeep K Reddy, Shelby C Straight, Pushp Bajaj, C Huy Pham, Marc Riera, Daniel R Moberg, Miguel A Morales, Chris Knight, Andreas W Götz, and Francesco Paesani. On the accuracy of the mb-pol many-body potential for water: Interaction energies, vibrational frequencies, and classical thermodynamic and dynamical properties from clusters to liquid water and ice. *The Journal of Chemical Physics*, 145(19):194504, 2016.

[123] Aleks Reinhardt and Bingqing Cheng. Quantum-mechanical exploration of the phase diagram of water. *Nature communications*, 12(1):588, 2021.

[124] Pengyu Ren and Jay W. Ponder. Polarizable atomic multipole water model for molecular mechanics simulation. *The Journal of Physical Chemistry B*, 107(24):5933–5947, 2003.

[125] Pengyu Ren and Jay W Ponder. Polarizable atomic multipole water model for molecular mechanics simulation. *The Journal of Physical Chemistry B*, 107(24):5933–5947, 2003.

[126] Luis Ruiz Pestana, Ondrej Marsalek, Thomas E. Markland, and Teresa Head-Gordon. The quest for accurate liquid water properties from first principles. *The Journal of Physical Chemistry Letters*, 9(17):5009–5016, 2018.

[127] Chitwan Saharia, William Chan, Saurabh Saxena, Lala Li, Jay Whang, Emily L Denton, Kamyar Ghasemipour, Raphael Gontijo Lopes, Burcu Karagol Ayan, Tim Salimans, et al. Photorealistic text-to-image diffusion models with deep language understanding. *Advances in neural information processing systems*, 35:36479–36494, 2022.

[128] Reza Salari, Thomas Joseph, Ruchi Lohia, Jérôme Hénin, and Grace Brannigan. A streamlined, general approach for computing ligand binding free energies and its application to gpcr-bound cholesterol. *Journal of chemical theory and computation*, 14(12):6560–6573, 2018.

[129] Ezry Santiago-McRae, Mina Ebrahimi, Jesse Sandberg, Grace Brannigan, and Jérôme Hénin. Computing absolute binding affinities by streamlined alchemical free energy perturbation [article v1. 0]. *Living Journal of Computational Molecular Science*, 5(1), 2023.

[130] Roland Schmid, Arzu M Miah, and Valentin N Sapunov. A new table of the thermodynamic quantities of ionic hydration: values and some applications (enthalpy–entropy compensation and born radii). *Physical Chemistry Chemical Physics*, 2(1):97–102, 2000.

[131] Kristof Schütt, Pieter-Jan Kindermans, Huziel Enoc Sauceda Felix, Stefan Chmiela, Alexandre Tkatchenko, and Klaus-Robert Müller. Schnet: A continuous-filter convolutional neural network for modeling quantum interactions. *Advances in neural information processing systems*, 30, 2017.

[132] Kristof T Schütt, Farhad Arbabzadah, Stefan Chmiela, Klaus R Müller, and Alexandre Tkatchenko. Quantum-chemical insights from deep tensor neural networks. *Nature communications*, 8(1):13890, 2017.

[133] Kristof T Schütt, Stefaan SP Hessmann, Niklas WA Gebauer, Jonas Lederer, and Michael Gastegger. Schnetpack 2.0: A neural network toolbox for atomistic machine learning. *The Journal of Chemical Physics*, 158(14), 2023.

[134] Thomas P Senftle, Sungwook Hong, Md Mahbubul Islam, Sudhir B Kylasa, Yuanxia Zheng, Yun Kyung Shin, Chad Junkermeier, Roman Engel-Herbert, Michael J Janik, Hasan Metin Aktulga, et al. The reaxff reactive force-field: development, applications and future directions. *npj Computational Materials*, 2(1):1–14, 2016.

[135] Khosrow Shakouri, JÃűrg Behler, JÃűrg Meyer, and Geert-Jan Kroes. Accurate neural network description of surface phonons in reactive gas–surface dynamics: N2+ ru (0001). *The journal of physical chemistry letters*, 8(10):2131–2136, 2017.

[136] Yue Shi, Pengyu Ren, Michael Schnieders, and Jean-Philip Piquemal. *Polarizable Force Fields for Biomolecular Modeling*, chapter 2, pages 51–86. John Wiley and Sons, Ltd, 2015.

[137] Yue Shi, Zhen Xia, Jiajing Zhang, Robert Best, Chuanjie Wu, Jay W Ponder, and Pengyu Ren. Polarizable atomic multipole-based amoeba force field for proteins. *Journal of Chemical Theory and Computation*, 9(9):4046–4063, 2013.

[138] Justin S Smith, Olexandr Isayev, and Adrian E Roitberg. Ani-1: an extensible neural network potential with dft accuracy at force field computational cost. *Chemical Science*, 8(4):3192–3203, 2017.

[139] Alan K Soper. The radial distribution functions of water as derived from radiation total scattering experiments: Is there anything we can say for sure? *International Scholarly Research Notices*, 2013, 2013.

[140] Robin J Speedy. Thermodynamic properties of supercooled water at 1 atm. *Journal of Physical Chemistry*, 91(12):3354–3358, 1987.

[141] Qiming Sun. Libcint: An efficient general integral library for gaussian basis functions. *Journal of Computational Chemistry*, 36(22):1664–1671, 2015.

[142] Qiming Sun, Timothy C. Berkelbach, Nick S. Blunt, George H. Booth, Sheng Guo, Zhendong Li, Junzi Liu, James D. McClain, Elvira R. Sayfutyarova, Sandeep Sharma, Sebastian Wouters, and Garnet Kin-Lic Chan. Pyscf: the python-based simulations of chemistry framework. *WIREs Computational Molecular Science*, 8(1):e1340, 2018.

[143] Qiming Sun, Xing Zhang, Samragni Banerjee, Peng Bao, Marc Barbry, Nick S. Blunt, Nikolay A. Bogdanov, George H. Booth, Jia Chen, Zhi-Hao Cui, Janus J. Eriksen, Yang Gao, Sheng Guo, Jan Hermann, Matthew R. Hermes, Kevin Koh, Peter Koval, Susi Lehtola, Zhendong Li, Junzi Liu, Narbe Mardirossian, James D. McClain, Mario Motta, Bastien Mussard, Hung Q. Pham, Artem Pulkin, Wirawan Purwanto, Paul J. Robinson, Enrico Ronca, Elvira R. Sayfutyarova, Maximilian Scheurer, Henry F. Schurkus, James E. T. Smith, Chong Sun, Shi-Ning Sun, Shiv Upadhyay, Lucas K. Wagner, Xiao Wang, Alec White, James Daniel Whitfield, Mark J. Williamson, Sebastian Wouters, Jun Yang, Jason M. Yu, Tianyu Zhu, Timothy C. Berkelbach, Sandeep Sharma, Alexander Yu. Sokolov, and Garnet Kin-Lic Chan. Recent developments in the pyscf program package. *The Journal of Chemical Physics*, 153(2):024109, 07 2020.

[144] Aidan P Thompson, H Metin Aktulga, Richard Berger, Dan S Bolintineanu, W Michael Brown, Paul S Crozier, Pieter J In't Veld, Axel Kohlmeyer, Stan G Moore, Trung Dac Nguyen, et al. Lammps-a flexible simulation tool for particle-based materials modeling at the atomic, meso, and continuum scales. *Computer Physics Communications*, 271:108171, 2022.

[145] Diata Traore, Olivier Adjoua, César Feniou, Ioanna-Maria Lygatsika, Yvon Maday, Evgeny Posenitskiy, Kerstin Hammernik, Alberto Peruzzo, Julien Toulouse, Emmanuel Giner, et al. Shortcut to chemically accurate quantum computing via density-based basis-set correction. *Communications Chemistry*, 7(1):269, 2024.

[146] Oliver T Unke, Stefan Chmiela, Michael Gastegger, Kristof T Schütt, Huziel E Sauceda, and Klaus-Robert Müller. Spookynet: Learning force fields with electronic degrees of freedom and nonlocal effects. *Nature Communications*, 12(1):1–14, 2021.

[147] Oliver T Unke and Markus Meuwly. Physnet: A neural network for predicting energies, forces, dipole moments, and partial charges. *Journal of Chemical Theory and Computation*, 15(6):3678–3693, 2019.

[148] David Van Der Spoel, Erik Lindahl, Berk Hess, Gerrit Groenhof, Alan E Mark, and Herman JC Berendsen. Gromacs: fast, flexible, and free. *Journal of Computational Chemistry*, 26(16):1701–1718, 2005.

[149] Kenno Vanommeslaeghe, Elizabeth Hatcher, Chayan Acharya, Sibsankar Kundu, Shijun Zhong, Jihyun Shim, Eva Darian, Olgun Guvench, P Lopes, Igor Vorobyov, et al. Charmm general force field: A force field for drug-like molecules compatible with the charmm all-atom additive biological force fields. *Journal of Computational Chemistry*, 31(4):671–690, 2010.

[150] Carlos Vega and Jose LF Abascal. Simulating water with rigid non-polarizable models: a general perspective. *Physical Chemistry Chemical Physics*, 13(44):19663–19688, 2011.

[151] Wolfgang Wagner and Andreas Pruß. The iapws formulation 1995 for the thermodynamic properties of ordinary water substance for general and scientific use. *Journal of physical and chemical reference data*, 31(2):387–535, 2002.

[152] Guangming Wang, Abdulgani Annaberdiyev, Cody A. Melton, M. Chandler Bennett, Luke Shulenburger, and Lubos Mitas. A new generation of effective core potentials from correlated calculations: 4s and 4p main group elements and first row additions. *The Journal of Chemical Physics*, 151(14):144110, 10 2019.

[153] Junmei Wang, Piotr Cieplak, and Peter A Kollman. How well does a restrained electrostatic potential (resp) model perform in calculating conformational energies of organic and biological molecules? *Journal of computational chemistry*, 21(12):1049–1074, 2000.

[154] Junmei Wang, Wei Wang, Peter A Kollman, and David A Case. Antechamber: an accessory software package for molecular mechanical calculations. *Journal of the American Chemical Society*, 222(1):2001, 2001.

[155] Junmei Wang, Romain M Wolf, James W Caldwell, Peter A Kollman, and David A Case. Development and testing of a general amber force field. *Journal of Computational Chemistry*, 25(9):1157–1174, 2004.

[156] Tong Wang, Xinheng He, Mingyu Li, Yatao Li, Ran Bi, Yusong Wang, Chaoran Cheng, Xiangzhen Shen, Jiawei Meng, He Zhang, et al. Ab initio characterization of protein molecular dynamics with ai2bmd. *Nature*, pages 1–9, 2024.

[157] Yanxing Wang, Théo Jaffrelot Inizan, Chengwen Liu, Jean-Philip Piquemal, and Pengyu Ren. Incorporating neural networks into the amoeba polarizable force field. *The Journal of Physical Chemistry B*, 128(10):2381–2388, 2024.

[158] Yuanqing Wang, Josh Fass, Benjamin Kaminow, John E Herr, Dominic Rufa, Ivy Zhang, Iván Pulido, Mike Henry, Hannah E Bruce Macdonald, Kenichiro Takaba, et al. End-to-end differentiable construction of molecular mechanics force fields. *Chemical Science*, 13(41):12016–12033, 2022.

[159] Zhi-Xiang Wang and Yong Duan. Solvation effects on alanine dipeptide: A mp2/cc-pvtz//mp2/6-31g** study of (ϕ, ψ) energy maps and conformers in the gas phase, ether, and water. *Journal of computational chemistry*, 25(14):1699–1716, 2004.

[160] Joseph L Watson, David Juergens, Nathaniel R Bennett, Brian L Trippe, Jason Yim, Helen E Eisenach, Woody Ahern, Andrew J Borst, Robert J Ragotte, Lukas F Milles, et al. De novo design of protein structure and function with rfdiffusion. *Nature*, 620(7976):1089–1100, 2023.

[161] Lan Yang, Jichen Li, Feiyang Chen, and Kuang Yu. A transferrable range-separated force field for water: Combining the power of both physically-motivated models and machine learning techniques. *The Journal of Chemical Physics*, 157(21):214108, 2022.

[162] Yinuo Yang, Shuhao Zhang, Kavindri D Ranasinghe, Olexandr Isayev, and Adrian E Roitberg. Machine learning of reactive potentials. *Annual Review of Physical Chemistry*, 75(1):371–395, 2024.

[163] Viktor Zaverkin and J Kästner. Gaussian moments as physically inspired molecular descriptors for accurate and scalable machine learning potentials. *Journal of Chemical Theory and Computation*, 16(8):5410–5421, 2020.

[164] Jinzhe Zeng, Duo Zhang, Denghui Lu, Pinghui Mo, Zeyu Li, Yixiao Chen, Marián Rynik, LiâĂŹang Huang, Ziyao Li, Shaochen Shi, et al. Deepmd-kit v2: A software package for deep potential models. *The Journal of Chemical Physics*, 159(5), 2023.

[165] Linfeng Zhang, Han Wang, Maria Carolina Muniz, Athanassios Z Panagiotopoulos, Roberto Car, and Weinan E. A deep potential model with long-range electrostatic interactions. *The Journal of Chemical Physics*, 156(12):124107, 2022.

[166] Shuhao Zhang, Małgorzata Z Makoś, Ryan B Jadrich, Elfi Kraka, Kipton Barros, Benjamin T Nebgen, Sergei Tretiak, Olexandr Isayev, Nicholas Lubbers, Richard A Messerly, et al. Exploring the frontiers of condensed-phase chemistry with a general reactive machine learning potential. *Nature Chemistry*, 16(5):727–734, 2024.

[167] Yukun Zhang, Xiaoming Zhang, Jinzhao Sun, Heng Lin, Yifei Huang, Dingshun Lv, and Xiao Yuan. Fault-tolerant quantum algorithms for quantum molecular systems: A survey. *arXiv preprint arXiv:2502.02139*, 2025.

[168] Xuanyu Zhu, Marc Riera, Ethan F Bull-Vulpe, and Francesco Paesani. Mb-pol (2023): Sub-chemical accuracy for water simulations from the gas to the liquid phase. *Journal of Chemical*

Theory and Computation, 2023.

[169] Juntang Zhuang, Tommy Tang, Yifan Ding, Sekhar C Tatikonda, Nicha Dvornek, Xenophon Papademetris, and James Duncan. Adabelief optimizer: Adapting stepsizes by the belief in observed gradients. *Advances in neural information processing systems*, 33:18795–18806, 2020.

[170] James F Ziegler and Jochen P Biersack. The stopping and range of ions in matter. In *Treatise on heavy-ion science: volume 6: astrophysics, chemistry, and condensed matter*, pages 93–129. Springer, 1985.

[171] Roman Zubatyuk, Justin S Smith, Jerzy Leszczynski, and Olexandr Isayev. Accurate and transferable multitask prediction of chemical properties with an atoms-in-molecules neural network. *Science advances*, 5(8):eaav6490, 2019.

[172] Roman Zubatyuk, Justin S. Smith, Jerzy Leszczynski, and Olexandr Isayev. Accurate and transferable multitask prediction of chemical properties with an atoms-in-molecules neural network. *Science Advances*, 5(8):eaav6490, 2019.

[173] Roman Zubatyuk, Justin S Smith, Benjamin T Nebgen, Sergei Tretiak, and Olexandr Isayev. Teaching a neural network to attach and detach electrons from molecules. *Nature Communications*, 12(1):1–11, 2021.